ENVISAT GOMOS Monthly report: March - September 2005

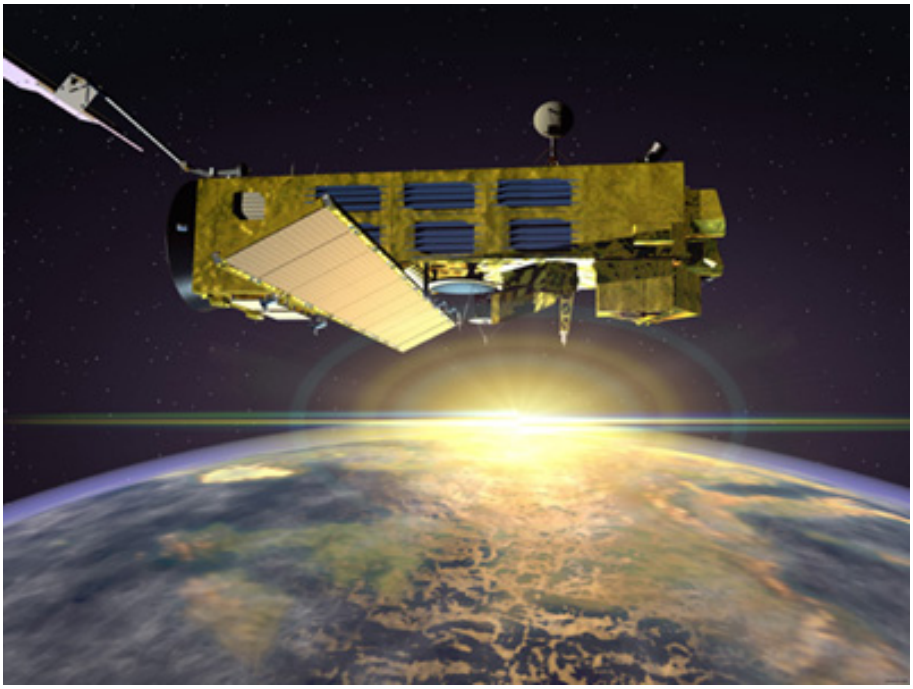

Prepared by:	L. Saavedra de Miguel - SERCO - GOMOS DPQC-EOO Team
Inputs from:	GOMOS Quality Working Group, ECMWF

Issue:	1.0
Reference:	ENVI-SPPA-EOPG-TN-05-0021
Date of issue:	28 October 2005
Status:	Reviewed
Document type:	Technical Note

Approved by:	Gilbert Barrot - ACRI - GOMOS DPQC-EOX Team

TABLE OF CONTENTS

1 INTRODUCTION

The GOMOS monthly report documents the current status and recent changes to the GOMOS instrument, its data processing chain, and its data products.
The Monthly Report (hereafter MR) is composed of analysis results obtained by the Data Processing and Quality Control, combined with inputs received from the different entities working on GOMOS operation, calibration, product validation and data quality. These teams participate in the GOMOS Quality Working Group:

- European Space Agency (ESRIN, ESOC, ESTEC-PLSO)
- DPQC
- ACRI
- Service d'Aeronomie
- Finnish Meteorological Institute
- IASB-Belgian Institute for Space Aeronomy
- Astrium Space
- ECMWF

In addition, the group interfaces with the Atmospheric Chemistry Validation Team.

1.1 Scope

The main objective of the Monthly Report is to give, on a regular basis, the status of GOMOS instrument performance, data acquisition, results of anomaly investigations, calibration activities and validation campaigns. The following six sections compose the MR:

- Summary
- Unavailability
- Instrument Configuration and Performance
- Level 1 Product Quality Monitoring
- Level 2 Product Quality Monitoring
- Validation Activities and Results

1.2 References

[1] ENVISAT Weekly Mission Operations Report #166, 167#, #168, #169, #170, #171 ENVI-ESOC-OPS-RP-1011-TOS-OF
[2] 'Level 1b Detailed Processing Model', PO-RS-ACR-GS-0001, issue 6.2, 21 Jun, 2005
[3] 'Level 2 Detailed Processing Model', PO-RS-ACR-GS-0002, issue 6.1, 21 Jun, 2005
[4] ECMWF GOMOS Monthly Reports

1.3 Acronyms and Abbreviations

ACVT	Atmospheric Chemistry Validation Team
ADF	Auxiliary Data File
ADS	Auxiliary Data Server
ANX	Ascending Node Crossing
ARB	Anomaly Review Board
ARF	Archiving Facility (PDS)
CCU	Central Communication Unit
CFS	CCU Flight Software
CNES	Centre National d'Études Spatiales
CTI	Configuration Table Interface / Configurable Transfer Item
CR	Cyclic Report
DC	Dark Charge
DMOP	Detailed Mission Operation Plan
DPM	Detailed Processing Model
DPQC	Data Processing and Quality Control
DS	Data Server
DSA	Dark Sky Area
DSD	Data Set Descriptor
ECMWF	European Centre for Medium Weather Forecast
EQSOL	Equipment Switch Off Line
ESA	European Space Agency
ESL	Expert Support Laboratory
ESRIN	European Space Research Institute
ESTEC	European Space Research & Technology Centre
ESOC	European Space Operations Centre
FCM	Fine Control Mode
FMI	Finnish Meteorological Institute
FOCC	Flight Operations Control Centre (ENVISAT)
FP1	Fast Photometer 1
FP2	Fast Photometer 2
GADS	Global Annotations Data Set
GOMOS	Global Ozone Monitoring by Occultation of Stars
GOPR	GOmos PRototype
GS	Ground Segment
HK	Housekeeping
IASB	Institut d'Aeronomie Spatiale de Belgique
IAT	Interactive Analysis Tool
ICU	Instrument Control Unit
IDL	Interactive Data Language
IECF	Instrument Engineering and Calibration Facilities
IMK	Institute of Meteorology Karlsruhe (Meteorologisch Institut Karlsuhe)
INV	Inventory Facilities (PDS)
IPF	Instrument Processing Facilities (PDS)
JPL	Jet Propulsion Laboratory
LAN	Local Area Network
LMA	Levenberg-Marquardt Algorithm

LPCE	Laboratoire de Physique et Chimie de l'Environnement
LUT	Look Up Table
MCMD	Macro Command
MDE	Mechanism Drive Electronics
MIP	Most Illuminated Pixel
MPH	Main Product Header
MPS	Mission Planning System
MR	Monthly Report
OBT	On Board Time
OCM	Orbit Control Manoeuvre
OOP	Out-of-plane
OP	Operational Phase of ENVISAT
PAC	Processing and Archiving Centre (PDS)
PCF	Product Control Facility
PDCC	Payload Data Control Centre (PDS)
PDHS	Payload Data Handling Station (PDS)
PDHS-E	Payload Data Handling Station – ESRIN
PDHS-K	Payload Data Handling Station – Kiruna
PDS	Payload Data Segment
PEB	Payload Equipment Bay
PLSOL	Payload Switch off Line
PMC	Payload Module Computer
PRNU	Pixel Response Non Uniformity
PSO	On-Orbit Position
QC	Quality Control
QUARC	Quality Analysis and Reporting Computer
QWG	Quality Working Group
RGT	ROP Generation Tool
RIVM	Rijksinstituut voor Volksgezondheid en Milieu
ROP	Reference Operations Plan
RTS	Random Telegraphic Signal
SA	Service d'Aeronomie
SAA	South Atlantic Anomaly
SATU	Star Acquisition and Tracking Unit
SFA	Steering Front Assembly
SFCM	Stellar Fine Control Mode
SFM	Steering Front Mechanism
SMNA	Servicio Meteorológico Nacional de Argentina
SODAP	Switch On and Data Acquisition Phase
SPA1	Spectrometer A CCD 1
SPA2	Spectrometer A CCD 2
SPB1	Spectrometer B CCD 1
SPB2	Spectrometer B CCD 2
SPH	Specific Product Header
SQADS	Summary Quality Annotation Data Set
SSP	Sun Shade Position
SZA	Solar Zenith Angle
VCCS	Voice Coil Command Saturation

2 SUMMARY

The GOMOS data measurements were suspended on 25th January 2005 following a major instrument anomaly: the instrument entered in Stand by / Refuse mode due to a failure in the "Elevation Voice coil" which is part of the Steering Front Mechanism. The anomaly occurs during the rallying of the telescope in the preparation for the star observation. After several months of anomaly investigations, GOMOS has been declared operational by the ARB since 29th August 2005. In order to provide an optimal operational service the azimuth field of view is reduced to a range between -5 to +20 degrees which means that around 60% of the starts that could be obtained with the full azimuth range are used for measurements. Anyway, star occultations could be lost due to a voice coil anomaly although in the new operational scenario (opposed to the original one) this does not lead to a suspended operation as the instrument now will try to find the subsequent star target. The modification in the operation strategy is also such that the maximum loss of consecutive observations cannot exceed two orbits. Further operation optimization by responsible scientists based in star properties and data processor specifications will result in an additional improvement of the dataset (section 3.1).

A summary of GOMOS testing and anomaly investigation operations since anomaly occurred on 25th January until 29th August 2005 is provided in section 4.1.

Data availability (when instrument was in operation): the decrease of data availability on the second week of August (8-15 Aug 2005) is because the nominal GOMOS operation was stopped for some testing on 12th August 2005 and was left in PAUSE mode until 18th August 2005. For the rest of the period the level 0 data availability is quite high while for level 1b the archived products have still relatively low statistics (section 3.3).

Temperatures: the CCD temperatures during March – September 2005 period present the expected global increase due to the radiator ageing. Another expected variation of the temperatures, the seasonal one, with amplitude of around 0.8 degree can also be observed (section 4.3).

Modulation signal: the standard deviation of the modulation signal presents high values during summer time for both 2004 and 2005 years for the ESRIN data, being now confirmed that the South Atlantic Anomaly is the cause of these unexpected peaks. The quality of ESRIN data, in particular over the SAA zone, is thus under investigation (section 4.5.2).

Star detection performance: the stars should be detected not far from the SATU center, that is, pixel number 145 in elevation and number 205 in azimuth. It has been observed that the azimuth MIP was within the threshold since September 2002 until the occurrence of the VCCS anomaly on January 2005. The reason for the change in trend observed after the anomaly is, at the moment, not understood. The elevation MIP had a significant variation until 12th December 2003 when a new PSO algorithm was activated in order to reduce the deviations of the ENVISAT platform attitude with respect to the nominal one. Similarly to the azimuth, after the anomaly of January 2005 the Elevation MIP has a drift that has no explanation. Investigations are on going to try to understand this behavior of the MIP that although does not impact the data quality, it may invalidate attitude monitoring by GOMOS and could represent a hidden anomaly (section 4.6.3).

Radiometric sensitivity monitoring: for star 25 and 9 the UV ratio is greater than the threshold 10%. It is clear that there is a global decrease of UV ratios for all the stars. This confirms the expected degradation suffered by the UV optics that is, anyway, very small considering also the small variation for the rest of the stars. For the photometers radiometric sensitivity ratios it is observed that every star has a variation that seems to be seasonal related. The variation is significant for stars 25 and 18. After some investigations performed by the QWG, it has been concluded that the problem is not linked to the photometers. A further indication that the problem is not on the photometer sensitivity is that every star has a very different behaviour (section 5.4.1).

Wavelength calibration: During the last wavelength calibration analysis performed using two occultations on 28th September 2005, the spectral shifts for SPA2 CCD were greater than 0.07 (warning value) and QWG has decided to recalibrate the wavelength assignment when the new processor GOMOS/5.00 will be ready (section 5.3).

Dark Charge calibration: new calibration ADF's (GOM_CAL_AX files) were disseminated during the reporting period with updated DC calibration maps (see dates and orbits used for the calibrations in section 5.1.2).

3 INSTRUMENT UNAVAILABILITY

3.1 GOMOS Unavailability Periods

In table 3.1-1 there is a list of GOMOS unavailability reports issued during the period 1st March until 30th September 2005. During the reporting period GOMOS was in no-measure the majority of the time due to a major anomaly: the "voice coil command saturation" anomaly.

The problem resulted from a failure in the telescope elevation drive, the so called "elevation voice coil", which is part of the Steering Front Mechanism. The anomaly occurs during the rallying of the telescope in the preparation for the star observation. In the original set-up this anomaly forced the instrument to switch down to Stand-by provoking an interruption of the operation until the error was recovered from the ground. The unavailability of the system became permanent as the anomaly immediately reappeared when the nominal procedures were applied.

A work-around solution put in place foresees that in case of a voice coil anomaly occurrence the instrument control unit (ICU) ignores the error, continues operation and rallies the telescope to the position for the following star observation. However, even with the work-around the error statistics show that 1 to 5 stars can be lost per orbit, in some cases this number can be much higher. This loss cannot be predicted based on the current status of the analysis. The overall operation strategy has been modified such that the maximum loss of consecutive observations cannot exceed two orbits.

Based on a series of tests (table 4.1-2), the ARB recommends limiting the rallying time to an equivalent maximum azimuth field of view of 20-25 degrees between one star and the following one and to operate the instrument in the azimuth range [-5, +20] degrees for some time in order to obtain significant experience and statistics in this reduced operational mode. This will yield about 19 stars per orbit, around 60% of the stars that could be obtained with the full azimuth range. At a later stage both the azimuth boundaries and range may be redefined.

Table 3.1-1: List of unavailability periods issued during the reporting period

Reference of unavailability report	Start time Star orbit	Stop time Stop orbit	Description
EN-UNA-2005/0243	5 Mar 2005 05:01:35 Orbit = 15747	18 Jul 2005 13:21:44 Orbit = 17685	GOMOS is in standby/refuse mode due to VCOIL CMDSAT
EN-UNA-2005/0282	12 Aug 2005 09:00:00 Orbit = 18040	12 Aug 2005 11:55:56 Orbit = 18042	Planned GOMOS SFM TEST as agreed by ARB
EN-UNA-2005/0298	12 Aug 2005 12:19:41 Orbit = 18042	18 Aug 2005 02:05:57 Orbit = 18122	GOMOS unavailable due to VOICE COIL ANOMALY
EN-UNA-2005/0355	7 Sep 2005 04:20:00 Orbit = 18409	7 Sep 2005 13:40:00 Orbit = 18415	Planned OCM and standby/refuse: The mirror should be moved to the SSP position prior to the Manoeuvre but the VCCS anomaly occurred and the "SSP not reached" status yielded GOMOS to go to Standby / Refuse

3.2 Stars Lost in Centering

The acquisition of a star initiates with a rallying phase where the telescope mechanism is directed towards the expected position of the star. Subsequently the acquisition procedure enters into detection mode, where the SATU star tracker output signal is pre-processed for spot presence survey and for the location of the most illuminated couple of adjacent pixels for two added lines, over the detection field. The Most Illuminated Pixel (MIP) defines the position of the first SATU centering window. The following step in the acquisition sequence is then initiated and consists of a centering phase where the SATU output signal is pre-processed for spot presence survey over the maximum of 10x10 pixel field. This allows the third phase to begin: the tracking phase.

The centering phase has occasionally resulted in loss of the star from the field of view. The fig. 3.2-1 reports the percentage of the stars lost in centering for the period 03-FEB-2003 to 25-SEP-2005. It can be seen that three stars, mainly weak stars (higher star id means higher magnitude) are lost during centering phase between 5 and 6 % of their planned observations. The star id 115 was lost 40% of the times but it was planned to be occulted five times and was lost twice (in period 19-25 January 2004), so this high percentage of loss is not statistically significant.

As the monitoring shows neither trend nor excessively high percentages of loss, there is no need for the moment to reject any star from the catalogue, and there is no indication of instrument-related problems.

Now with the instrument in a new operation scenario the stars are also lost due to the anomaly "elevation voice coil command saturation" even if the instrument is not going anymore to stand by / Refuse mode (see section 3.1). Monitoring the statistics of stars lost due to this anomaly maybe interesting not only to know the failure rate but also the impact it has to the dataset availability. The need of this routine monitoring and its set up will be studied in the following months.

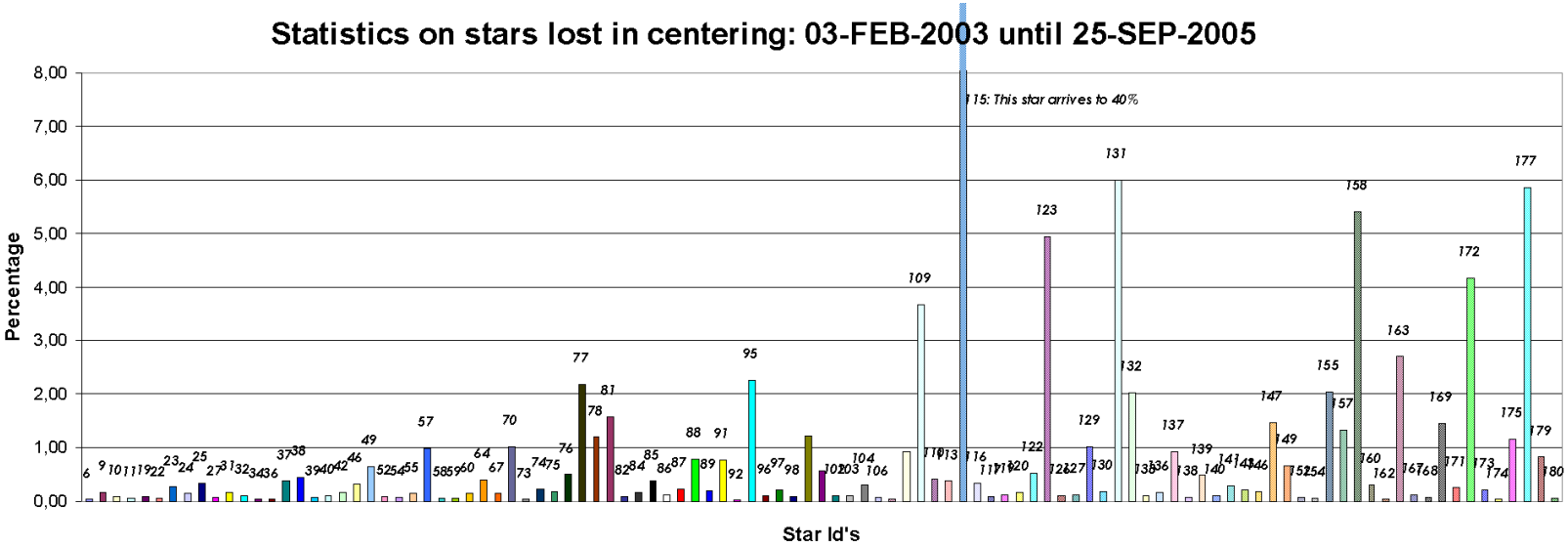

Figure 3.2-1: Statistics on stars that have been lost during the centering phase. The number above the columns correspond to the Star ID

3.3 Data Generation Gaps

The trend in percentage of available data within the archives PDHS-K and PDHS-E is depicted in fig. 3.3-1 (when instrument was in operation). It is a good indicator on how the PDS chain is working in terms of generation and dissemination of data to the archives. The percentage is calculated once per week.

The decrease of data availability on the second week of August (8-15 Aug 2005) is because the nominal GOMOS operation was stopped for some testing on 12th August 2005 and was left in PAUSE mode until 18th August 2005. For the rest of the period the level 0 data availability is quite high while for level 1b the archived products have still relatively low statistics.

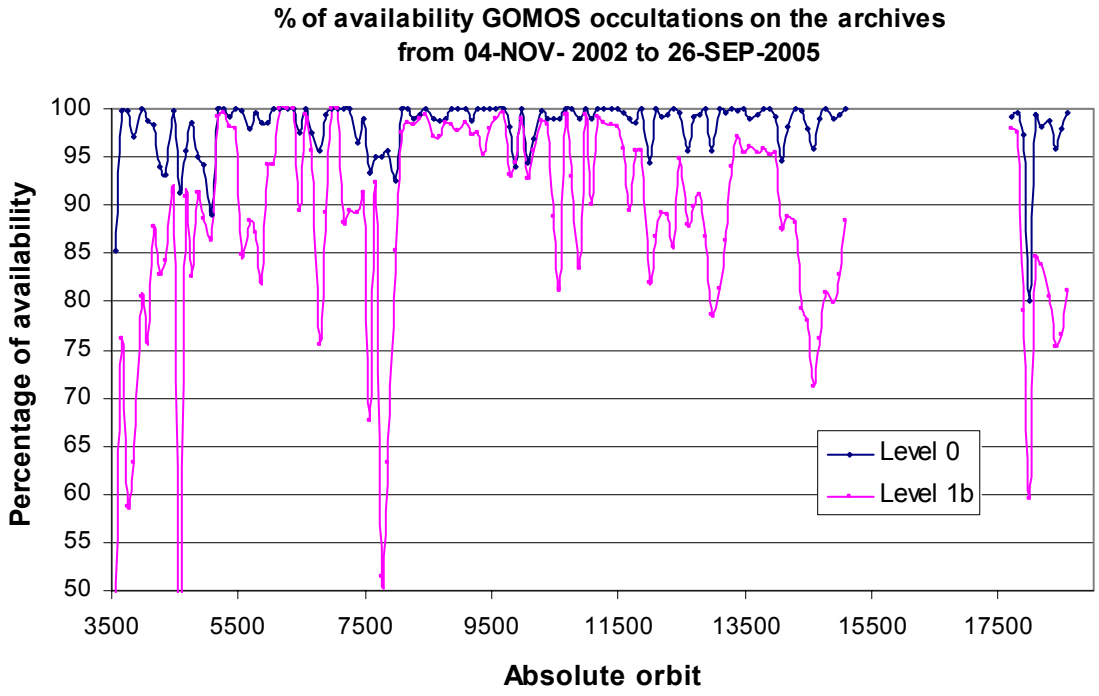

Figure 3.3-1: Percentage of level 0 and level 1b data availability on the archives PDHS-E and PDHS-K

3.3.1 LEVEL 0 PRODUCTS: GOM_NL__0P

Occultations planned to be acquired but for which no GOM_NL__0P data product has become available are presented in fig. 3.3-2 for the reporting period.

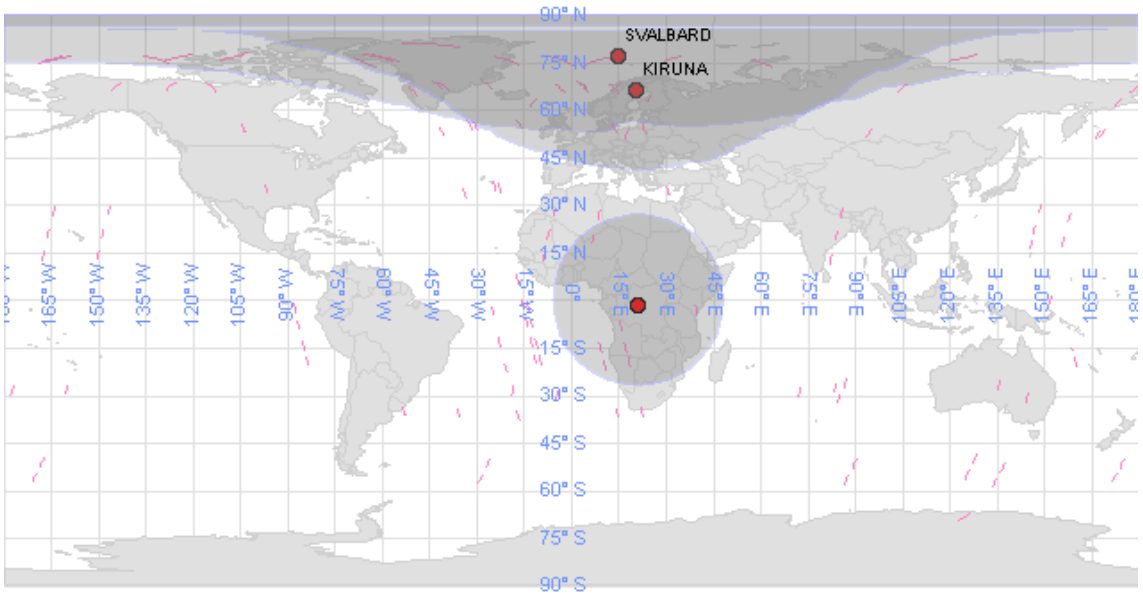

Figure 3.3-2: The pink lines are the orbit segments corresponding to planned data acquisitions for which no GOMOS level 0 product has become available. The grey shadows centered in Kiruna and Svalbard represents the visibility of those acquisition stations while the point over Africa represents the nominal position of ARTEMIS satellite

3.3.2 HIGHER LEVEL PRODUCTS

Routine dissemination of higher-level products produced by the PDS to the users is enabled. Year 2003 data (level 2) reprocessed by the processor developed and operated by ACRI are available (see section 6.1.3). A new reprocessing activity with the latest prototype version is on-going for the years 2002, 2003 and 2004. The next operational processor (actual is GOMOS 4.02, next one will be GOMOS/5.00) that generates data in near real time will be in line with the prototype used for the last reprocessing.

4 INSTRUMENT CONFIGURATION AND PERFORMANCE

4.1 Instrument Operation and Configuration

During the period end of March 2003 to July 2003 the azimuth range had to be decreased in steps (table 4.1-1) to avoid an instrument problem ("Voice_coil_command_saturation" anomaly) that caused GOMOS to go into STAND BY/REFUSE mode. On July 2003 the driver assembly was switched to the redundant B-side and since that date the full azimuth range (-10.8, +90.8) was again available until the second major anomaly occurred on 25th January 2005. Between this date and until the instrument is declared operational again (29th August 2005), GOMOS has been operated for testing and anomaly investigation purposes (table 4.1-2) in different GOMOS operations scenarios (table 4.1-3).

Table 4.1-1: Historical changes in Azimuth configuration when GOMOS operational

Date	Orbit	Minimum Azimuth	Maximum Azimuth
29-MAR-2003 17:40	5635	0.0	+90.8
31-MAY-2003 06:22	6530	+4.0	+90.8
16-JUN-2003 16:17	6765	+12.0	+90.8
15-JUL-2003 01:39	7200	-10.8	+90.8
25-JAN-2005 23:33	15200	tests	tests
29-AUG-2005 02:52	18280	-10	+10
26-SEP-2005 01:32	18680	-5	+20
03-OCT-2005 01:12	18780	-5	+15
09-OCT-2005 21:30	18878	-5	+20

Table 4.1-2: GOMOS testing and anomaly investigation operations since anomaly occurred on 25 JAN 2005. Every DSA for testing had duration of 100 seconds. Pink: anomaly; Green: working; Yellow: criticality patch uploaded

UTC time	Orbit	Mode (Asynchronous or Synchronous)	Operations and anomaly occurrences
15-FEB-2005 08:50:20	15492	A	1 DSA for testing
15-FEB-2005 10:25:30	15493	A	10 DSA for testing
22-FEB-2005 11:54:24	15594	A	Nominal SFA calibration: az=40
22-FEB-2005 15:07:30	15596	A	5 DSA for testing
22-FEB-2005 16:31:30	15597	A	9 DSA for testing
03-MAR-2005 23:26:02	15730	S	GOMOS picked up the nominal planning operations (see table 4.1-3)
05-MAR-2005 05:01:35	15747	S	VCCS Anomaly during nominal planning
08-MAR-2005 09:35:04	15793	A	VCCS Anomaly during nominal SFA calibration
11-MAR-2005 12:31:05	15838	A	VCCS Anomaly during nominal SFA calibration
22-MAR-2005 20:09:22	16000	S	GOMOS in 'non nominal 1' operations (see table 4.1-3)
22-MAR-2005 20.09.37	16000	S	VCCS Anomaly during 'non nominal 1' operations (see table 4.1-3)
08-APR-2005 19:48:00	16243	A	SFA calibration at az=0 (and El=65) 45 DSA for testing
11-APR-2005 11:19:29	16281	A	45 DSA for testing
12-APR-2005 09:04:29	16294	A	585 DSA for testing
15-APR-2005 00:20:33	16331	A	VCCS Anomaly during DSA measurements for testing
18-APR-2005 11:02:41	16381	-	VCCS Anomaly when switching on the MDE
19-APR-2005 07:30:18	16393	-	VCCS Anomaly when switching on the MDE
25-APR-2005 14:23:03	16483	-	VCCS Anomaly during nominal SFA calibration
02-MAY-2005 12:26:03	16582	-	VCCS Anomaly during nominal SFA calibration
09-JUN-2005 12:32:44	17126	-	SFA Criticality Patch uploaded: the scope is that COMOS does not switch down to REFUSE mode when VCCS occurs, but just skip the star and measures the following one
09-JUN-2005 15:48:35	17128	-	Anomaly requesting the PMC to switch-off the GOMOS ICU during nominal SFA calibration
17-JUN-2005 10:02:00	17239	A	3 DSA for testing
17-JUN-2005 11:37:30	17240	A	9 DSA for testing
20-JUN-2005 14:40:39	17285	A	1 orbit Occultation of real Stars with GOMOS in "non nominal 2" operations (see table 4.1-3) for testing
22-JUN-2005 08:35:43	17310	S	2 Synchronous sequence (5 orbits each) of Occultation of

			real stars with GOMOS in "non nominal 2" operations (see table 4.1-3) for testing
24-JUN-2005 10:54:47	17340	S	2 Synchronous sequence (5 orbits each) of Occultation of real stars with GOMOS in "non nominal 2" operations (see table 4.1-3) for testing
27-JUN-2005 14:15:20	17384	S	2 Synchronous sequence (5 orbits each) of Occultation of real stars with GOMOS in "non nominal 2" operations (see table 4.1-3) for testing
18-JUL-2005 13:21:44	17685	S	GOMOS picked up the 'non nominal 2' operations (see table 4.1-3)
12-AUG-2005 09:02:30	18040	A	VCCS Anomaly during DSA measurements for testing
12-AUG-2005 10:40:00	18041	A	VCCS Anomaly during DSA measurements for testing
12-AUG-2005 13:55:00	18043	A	9 DSA for testing
18-AUG-2005 01:58:03	18122	S	GOMOS picked up the 'non nominal 7' operations (see table 4.1-3)
29-AUG-2005 02:52:40	18280	S	GOMOS declared operational again, in 'non nominal 4' operations (see table 4.1-3)

Table 4.1-3: GOMOS planned operations generated by RGT for period March – September 2005. The planning is built on a 5-orbit sequences basis (5 orbits with the same stars) until 25 July 2005, when it is changed to a 2-orbit sequences basis. In red, the changes with respect to the previous generated planning

Planning	UTC Start	UTC stop	Star Id range	Limb	Az range (°)	El range (°)	Alt range (Km)
Mission interrupted	28-FEB-2005 11:35:47	03-MAR-2005 23:25:43	-	-	-	-	-
Nominal	03-MAR-2005 23:25:43	22-MAR-2005 20:07:24	Nominal: all in catalog	Nominal: all	Nominal: [-10, 90]	Nominal: [65, 62.5]	Nominal: [130, 5]
Non nominal 1	22-MAR-2005 20.07.24	18-APR-2005 09:14:56	Reduced: [1, 70]	Reduced: dark	Nominal: [-10, 90]	Extended: [68, 62.5]	Extended: [280, 5]
Mission interrupted	18-APR-2005 09:14:56	20-JUN-2005 06:13:52	-	-	-	-	-
Non nominal 2	20-JUN-2005 06:13:52	02-JUL-2005 03:15:39	Nominal: all in catalog	Nominal: all	Reduced: [-10, 10]	Extended: [68, 62.5]	Extended: [280, 5]
Mission interrupted	02-JUL-2005 03:15:39	04-JUL-2005 03:53:01	-	-	-	-	-
Non nominal 2	04-JUL-2005 05:33:37	25-JUL-2005 04:33:15	Nominal: all in catalog	Nominal: all	Reduced: [-10, 10]	Extended: [68, 62.5]	Extended: [280, 5]
Non nominal 3	25-JUL-2005 04:33:16	01-AUG-2005 04:13:08	Nominal: all in catalog	Nominal: all	Reduced: [-10, 10]	Extended: [66.7, 62.5]	Extended: [210, 5]
Non nominal 4	01-AUG-2005 04:13:08	08-AUG-2005 03:53:01	Nominal: all in catalog	Nominal: all	Reduced: [-10, 10]	Nominal: [65, 62.5]	Nominal: [130, 5]
Non nominal 5	08-AUG-2005 03:53:01	15-AUG-2005 03:32:54	Nominal: all in catalog	Nominal: all	Reduced: [-10, 20]	Nominal: [65, 62.5]	Nominal: [130, 5]
Non nominal 6	15-AUG-2005 03:32:54	18-AUG-2005 01:58:03	Nominal: all in catalog	Nominal: all	Reduced: [-10, 30]	Nominal: [65, 62.5]	Nominal: [130, 5]
Non nominal 7	18-AUG-2005 01:58:03	20-AUG-2005 00:54:03	Nominal: all in catalog	Nominal: all	Reduced: [0, 15]	Nominal: [65, 62.5]	Nominal: [130, 5]
Non nominal 8	20-AUG-2005 00:54:49	22-AUG-2005 03:12:46	Nominal: all in catalog	Nominal: all	Reduced: [15, 30]	Nominal: [65, 62.5]	Nominal: [130, 5]
Non nominal 9	22-AUG-2005 03:12:46	24-AUG-2005 02:09:33	Nominal: all in catalog	Nominal: all	Reduced: [30, 45]	Nominal: [65, 62.5]	Nominal: [130, 5]
Non nominal 10	24-AUG-2005 02:09:33	26-AUG-2005 01:06:18	Nominal: all in catalog	Nominal: all	Reduced: [45, 60]	Nominal: [65, 62.5]	Nominal: [130, 5]
Non nominal 4	26-AUG-2005 01:06:18	26-SEP-2005 01:32:10	Nominal: all in catalog	Nominal: all	Reduced: [-10, 10]	Nominal: [65, 62.5]	Nominal: [130, 5]

Non nominal 11	26-SEP-2005 01:32:10	03-OCT-2005 01:12:04	Nominal: all in catalog	Nominal: all	Reduced: [-5, 20]	Nominal: [65, 62.5]	Nominal: [130, 5]
Non nominal 12	03-OCT-2005 01:12:04	09-OCT-2005 21:30:45	Nominal: all in catalog	Nominal: all	Reduced: [-5, 15]	Nominal: [65, 62.5]	Nominal: [130, 5]
New scenario	09-OCT-2005 21:30:45	17-OCT-2005 00:31:49	Nominal: all in catalog	Nominal: all	Reduced: [-5, 20]	Nominal: [65, 62.5]	Nominal: [130, 5]

There was no new Configurable Table Interface (CTI) uploaded to the instrument. The files used since the beginning of the mission are in table 4.1-4.

Table 4.1-4: Historic CTI Tables

CTI filename	Dissemination to FOCC
CTI_SMP_GMVIEC20030716_123904_00000000_00000004_20030715_000000_20781231_235959.N1	16-JUL-2003
CTI_SMP_GMVIEC20021104_075734_00000000_00000003_20021002_000000_20781231_235959.N1	06-NOV-2003
CTI_SMP_GMVIEC20021002_082339_00000000_00000002_20021002_000000_20781231_235959.N1	07-OCT-2003
CTI_SMP_GMVIEC20020207_154455_00000000_00000000_20020301_032709_20781231_235959.N1	21-FEB-2002

4.2 Limb, Illumination conditions and instrument gain setting

The **limb** and the **illumination condition** are two parameters that can confuse the user community. In table 4.2-1 there are specified the product parameter (level 1b and level 2 of operational processor GOMOS/4.02) where the flag is located, the meaning and the source. The difference between the limb (SPH/bright_limb) and the illumination condition (SUMMARY_QUALITY/limb_flag) is that the first one is coming from the mission scenario and the second is coming from the processing (sun zenith angle computed). The SPH/bright_limb is for some occultations set to "dark" in the mission scenario while they are in fact in bright limb illumination conditions. To select highest quality data for scientific application, data with SUMMARY_QUALITY/limb_flag equal to '0' should be used (see also the disclaimer: http://envisat.esa.int/dataproducts/availability/disclaimers). The instrument gain settings are also specified in table 4.2-1 (they depend on the mission scenario flags) just for information completeness.

Table 4.2-1: Relationship between limb, illumination condition flags and instrument gain settings (operational IPF version GOMOS/4.02)

Products parameter	SPH/bright_limb	0 = Dark	1 = Bright	Coming from mission scenario
	SUMMARY_QUALITY/limb_flag	0 = Full Dark 1 = Bright 2 = Twilight	1 = Bright 2 = Twilight	In the geolocation process the sun zenith angle is computed and the occultation then is flagged accordingly
Instrument Gain	SPA Gain	3 (2)	0	Gain setting for spectrometer A. In parenthesis, values valid only for Sirius occultations (starID=1)
	SPB Gain	0	0	Gain setting for spectrometer B

The same is valid for the prototype version GOPR_6.0a_6.0a and following ones (including the one that is used for the on-going second reprocessing of 2002-2005 years), where the **limb** is in fields SPH/bright_limb and SUMMARY_QUALITY/dark_bright_limb and the **illumination condition** is in field SUMMARY_QUALITY/obs_ill_cond. For these prototypes, the illumination condition can have five values (see table 4.2-2).

Table 4.2-2: Relationship between limb, illumination condition flags and instrument gain settings (prototype version GOPR 6.0a_6.0a and following ones)

Products parameter	SPH/bright_limb SUMMARY_QUALITY/dark_bright_limb	0 = Dark	1 = Bright	Coming from mission scenario
	SUMMARY_QUALITY/obs_ill_cond	0 = Full Dark 1 = Bright 2 = Twilight 3 = Straylight 4 = Twi.+Stray.		In the geolocation process the sun zenith angle is computed and the occultation then is flagged accordingly
Instrument Gain	SPA Gain	3 (2)	0	Gain setting for spectrometer A. In parenthesis, values valid only for Sirius occultations (starID=1)
	SPB Gain	0	0	Gain setting for spectrometer B

4.3 Thermal Performance

Since the beginning of the mission the hot pixel and RTS phenomena are producing a continuous increase of the dark charge signal within the CCD detectors (see section 4.5.1). In order to minimize this effect, three successive CCD cool down were performed in orbits 800 (25th April 2002), 1050 (13th May 2002) and 2780 (11th September 2002) with a total decrease in temperature of 14 degrees.

Fig. 4.3-1 and 4.3-2 display, respectively, the overall temperature variation and the temperature variation around the Ascending Node Crossing (ANX) time with a resolution of 0.4 degrees (coding accuracy for level 0 data). The CCD temperatures during March – September 2005 period, present the expected global increase due to the radiator ageing. Another expected variation of the temperatures, the seasonal one, with amplitude of around 0.8 degree can be also observed. The peaks that occur mainly in spectrometer B1 and B2 are also to be noted. They happen a little before the ANX for some consecutive orbits and every 8-10 days. Their origin is still not known, as we did not find any correlation between these peaks and other activities carried out by other ENVISAT instruments. The CCD temperature at almost the same latitude location (fig. 4.3-2) is monitored in order to detect any inter-orbital temperature variation.

The abnormal decreases observed some times in all detectors are after GOMOS switch off periods, when the instrument did not have enough time to reach the nominal temperature before starting the measurements.

During September 2005, the orbital temperature variation of the detector SPB2 for ascending passes (fig. 4.3-3) is nominal, around 2.5 degrees. For descending passes (fig. 4.3-4) it arrives to 3.3 due to the GOMOS switch off on 7th September. The stability of the temperature during the orbit is important because it affects

the position of the interference patterns. The phenomenon of the interference is present mainly in SPB and this Pixel Response Non-Uniformity (PRNU) is corrected during the processing.

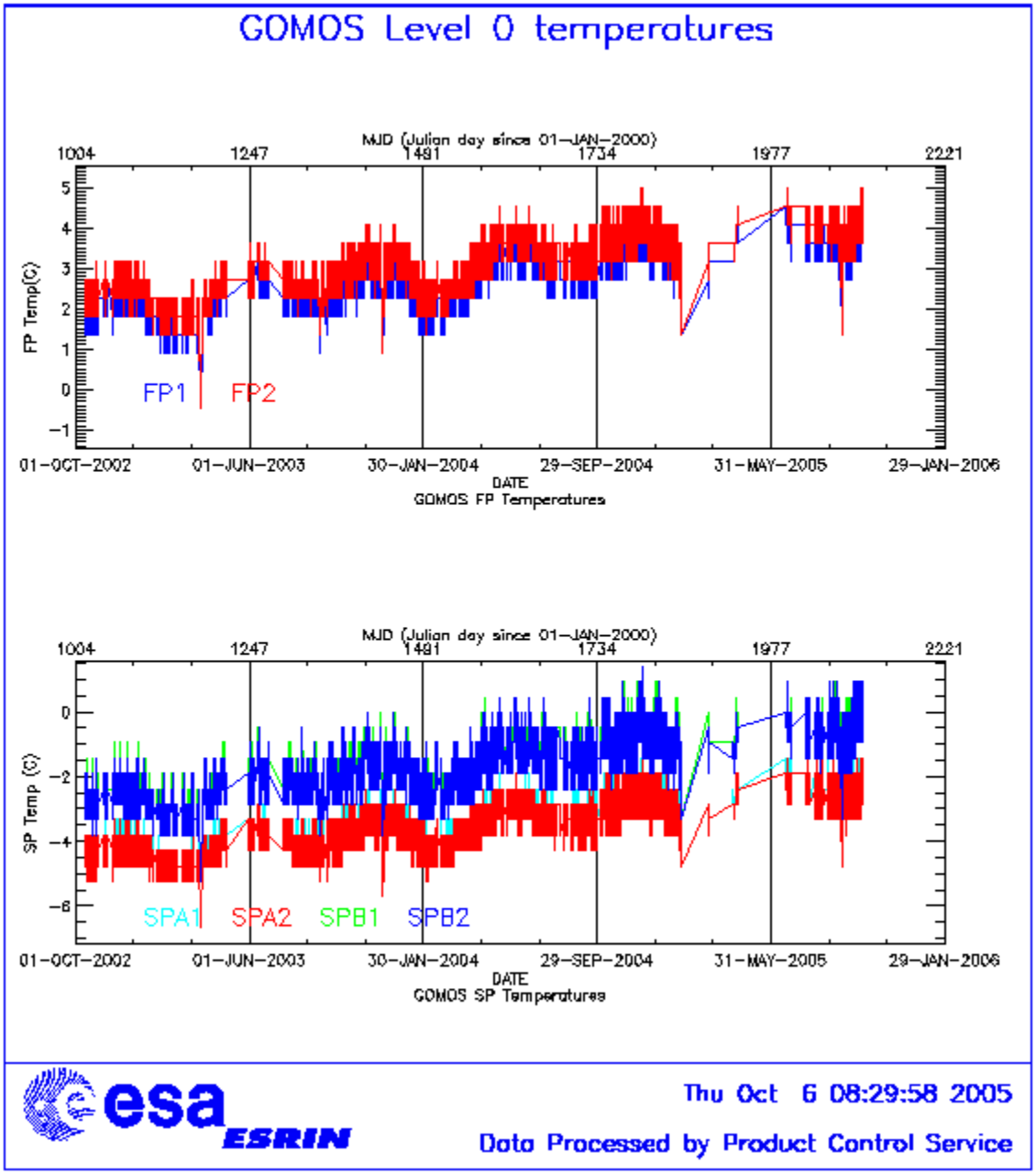

Figure 4.3-1: Level 0 temperature evolution of all GOMOS CCD detectors since October 2002 until the end of the reporting period

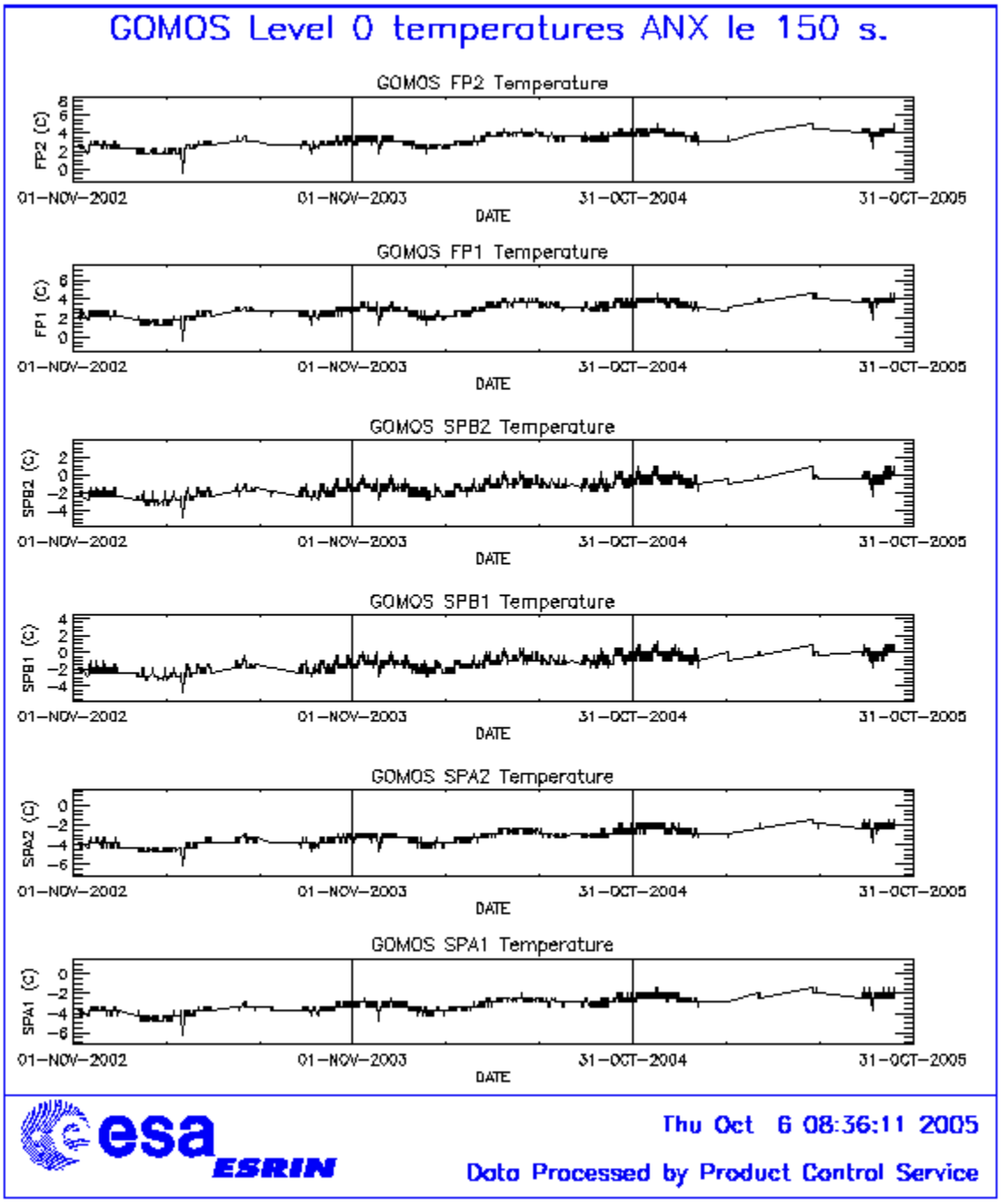

Figure 4.3-2: **Level 0 temperature evolution of all GOMOS CCD detectors around ANX since November 2002 until the end of the reporting period**

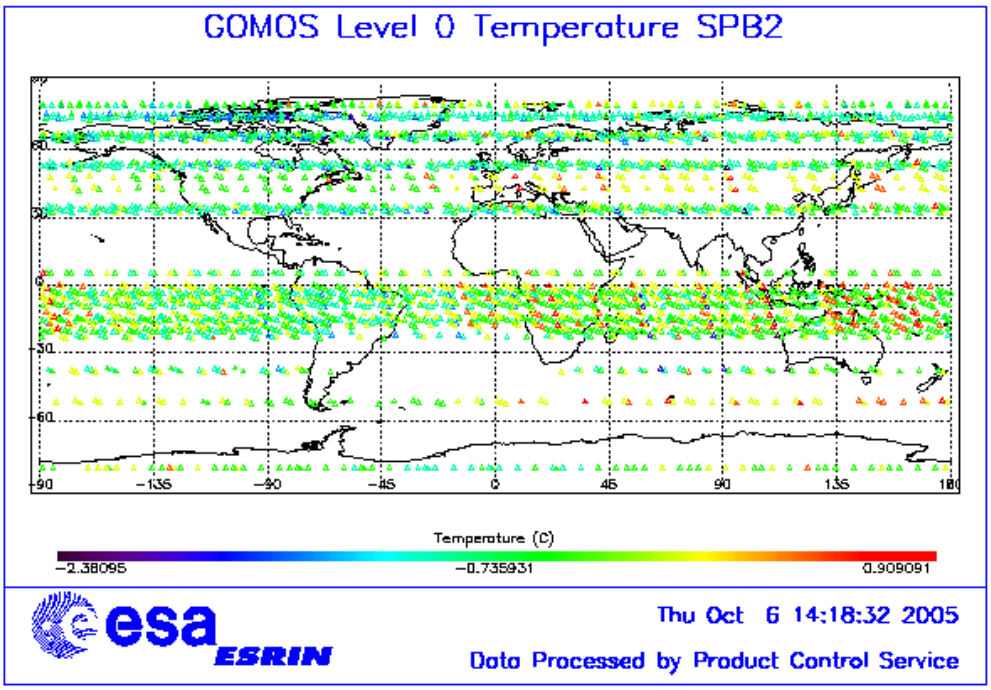

Figure 4.3-3: Ascending orbital variation of SPB2 temperature during reporting period

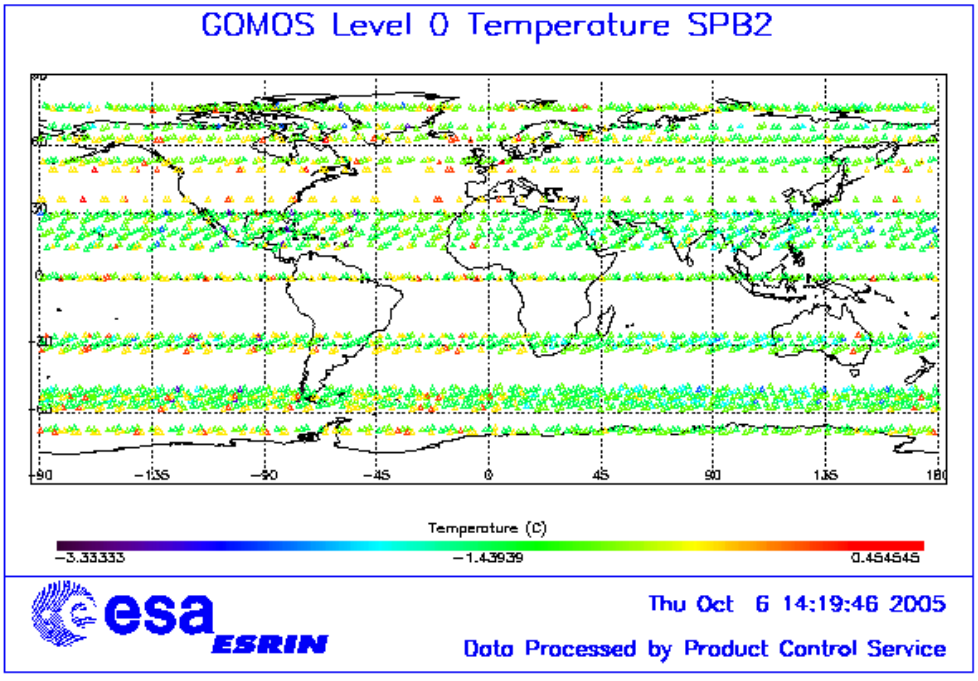

Figure 4.3-4: Descending orbital variation of SPB2 temperature during reporting period

4.4 Optomechanical Performance

No new band setting calibration has been performed during the reporting period. The last one has been done on April 2005.

- Version GOMOS/4.00 and previous ones:

In the processors versions of GOMOS GOMOS/4.00 and previous the spectra is expected to be aligned along CCD lines, and therefore use only a single average line index per CCD. In table 4.4-1 the mean values of the location of the star signal for all the calibration analysis done are reported. The 'left' and 'right' values are calculated (the whole interval is not used) because the spectra present a slight slope, more pronounced in the spectrometer B (see fig. 4.4-1). In table 4.4-2, mean values of the location of the star signal are calculated for some specific wavelength intervals. These intervals have been changed between the calibration performed in September 2002 and the ones performed afterwards (until November 2003). Table 4.4-3 reports the average location of the star spot on the photometer 1 and 2 CCD.

- Version GOMOS/4.02:

In the actual processor version (GOMOS/4.02) operational since 23rd March 2004, a Look Up Table (LUT) gives the line index of the spectra location as a function of the wavelength (blue dots in fig. 4.4-1). A new calibration exercise has been performed during April. The position of the stellar spectra of star id 31, 18 and 4 observed in dark-limb spatial spread monitoring mode have been averaged above 120 km altitude and compared to the values of the LUT. The results confirm the LUT values (see table 4.4-4) so for the time being there is no need to update the LUT.

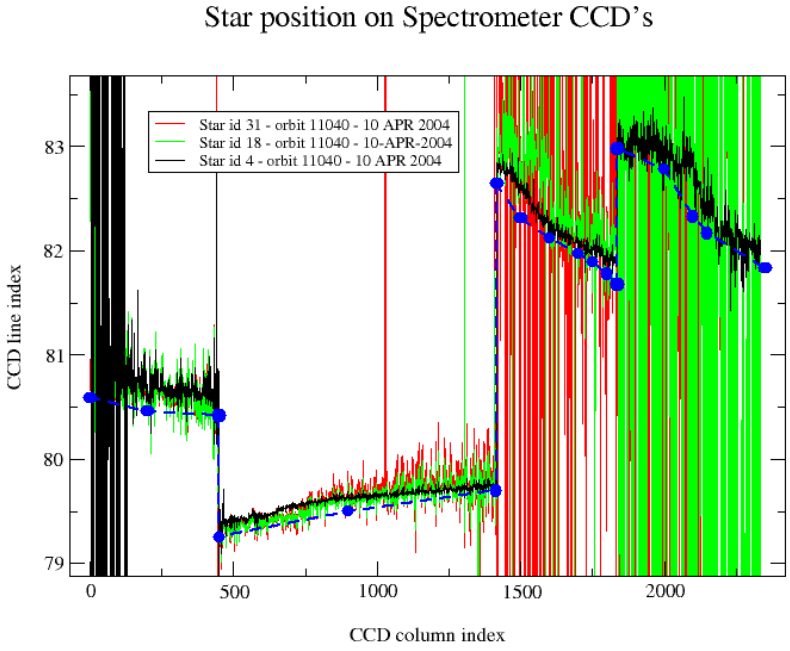

Figure 4.4-1: Average position of star spectra on the CCD

Table 4.4-1: Mean value of the location of the star signal during the occultation at the edges of every band (mean over 50 values, filtering the outliers)

	UV (SPA1) left/right	VIS (SPA2) left/right (Inverted spectra)	IR1 (SPB1) left/right	IR2 (SPB2) left/right
11/09/2002	80.7/80.7	79.8/79.5	82.8/81.9	83.1/82.1
01/01/2003	80.7/80.6	79.8/79.5	82.8/82.0	83.2/82.2
17/07/2003 & 02/08/2003	80.7/80.7	79.8/79.5	82.8/81.9	83.1/82.1
08/11/2003	80.7/80.6	79.8/79.5	82.8/81.9	83.1/82.1

Table 4.4-2: Mean value of the location of the star signal during the occultation (as table 4.4-1) but now within some wavelength intervals

	UV (SPA1)	VIS (SPA2)	IR1 (SPB1)	IR2 (SPB2)
11/09/2002 wl range (nm)	80.8 [300-330]	79.8 [500-530]	82.6 [760-765]	82.9 [937-942]
01/01/2003 wl range (nm)	80.6 [350-360]	78.6 [650-670]	81.6 [760-765]	80.3 [935-945]
02/08/2003	80.6	79.7	82.5	82.8
08/11/2003	80.6	79.9	82.4	82.8

Table 4.4-3: Average column and row pixel location of the star spot on the photometer CCD during the occultation

	FP1 (column/row)	FP2 (column/row)
11/09/2002	11/4	5/5
01/01/2003	10/4	6/4.9
02/08/2003	10/4	6/5
08/11/2003	10/4	6/5

Table 4.4-4: Location of the star signal on the CCD's (corresponding to fig. 4.4-1)

Pixel Column	LUT (Pixel line)	Calibration on 10-APR-2004
0	**80.59**	80.80
20	**80.46**	80.60
449	**80.42**	80.50
450	**79.25**	79.39
900	**79.50**	79.63
1415	**79.70**	79.76
1416	**82.64**	82.80
1500	**82.31**	82.60
1600	**82.12**	82.22
1700	**81.97**	82.04
1750	**81.89**	81.98
1800	**81.78**	81.91
1835	**81.68**	81.88
1836	**82.98**	83.10
2000	**82.78**	82.90
2100	**82.33**	82.70

2150	**82.17**	82.40
2350	**81.83**	82.00

4.5 Electronic Performance

4.5.1 DARK CHARGE EVOLUTION AND TREND

The trend of Dark Charge (DC) is of crucial importance for the final quality of the products, and is therefore subject to intense monitoring. As part of the DC there is:

- "Hot pixels", a pixel is "hot" when its dark charge exceeds its value measured on ground, at the same temperature, by a significant amount.
- RTS phenomenon (Random Telegraphic Signal), it is an abrupt change (positive or negative) of the CCD pixel signal, random in time, affecting only the DC part of the signal and not the photon generated signal.

The temperature dependence of the DC would make this parameter a good indicator of the DC behaviour, but the hot pixels and the RTS are producing a continuous increase of the DC (see trend in fig. 4.5-1 and 4.5-2). To take into account these phenomena, since version GOMOS/4.00 (actual one is GOMOS/4.02) a DC map per orbit is extracted from a Dark Sky Area (DSA) observation performed around ANX (full dark conditions). For every level 1b product (occultation), the actual thermistor temperature of the CCD is used to convert the DC map measured around ANX into an estimate of the DC at the time (and different temperature) of the actual occultation. When the DSA observation is not available, the DC map inside the calibration product that was measured at a given thermistor reference temperature is used; again, the actual thermistor temperature of the CCD is used to compute the actual map. Table 4.5-1 reports the list of products that used the DC maps inside the calibration file due to the non-availability of DSA observation. A "CAL DC map with no T dep." means that, as the temperature information was not available for that occultation, the DC map used is exactly the one inside the Calibration product.

Table 4.5-1: Table of level 1b products that used the Calibration DC maps instead of the DSA observation

Product name	DC information
GOM_TRA_1PNPDE20050903_203630_000000452040_00272_18362_0000.N1	DC map used
GOM_TRA_1PNPDE20050903_204011_000000422040_00272_18362_0001.N1	DC map used
GOM_TRA_1PNPDE20050903_204300_000000392040_00272_18362_0002.N1	DC map used
GOM_TRA_1PNPDE20050903_210327_000000352040_00272_18362_0003.N1	DC map used
GOM_TRA_1PNPDE20050903_210523_000000342040_00272_18362_0004.N1	DC map used
GOM_TRA_1PNPDE20050903_210637_000000372040_00272_18362_0005.N1	DC map used
GOM_TRA_1PNPDE20050903_211910_000000362040_00272_18362_0006.N1	DC map used
GOM_TRA_1PNPDE20050904_200456_000000382040_00286_18376_0000.N1	DC map with no T dep.
GOM_TRA_1PNPDE20050904_200837_000000402040_00286_18376_0001.N1	DC map used
GOM_TRA_1PNPDE20050904_201126_000000392040_00286_18376_0002.N1	DC map used
GOM_TRA_1PNPDE20050904_203152_000000352040_00286_18376_0003.N1	DC map used
GOM_TRA_1PNPDE20050905_024146_000000382040_00290_18380_0000.N1	DC map with no T dep.
GOM_TRA_1PNPDE20050905_024720_000000402040_00290_18380_0001.N1	DC map used
GOM_TRA_1PNPDE20050905_025101_000000432040_00290_18380_0002.N1	DC map used

GOM_TRA_1PNPDE20050905_025350_000000372040_00290_18380_0003.N1	DC map used
GOM_TRA_1PNPDE20050905_031415_000000352040_00290_18380_0004.N1	DC map used
GOM_TRA_1PNPDE20050905_031612_000000372040_00290_18380_0005.N1	DC map used
GOM_TRA_1PNPDE20050905_031725_000000382040_00290_18380_0006.N1	DC map used
GOM_TRA_1PNPDE20050905_193322_000000382040_00300_18390_0000.N1	DC map with no T dep.
GOM_TRA_1PNPDE20050905_193703_000000402040_00300_18390_0001.N1	DC map used
GOM_TRA_1PNPDE20050905_193951_000000402040_00300_18390_0002.N1	DC map used
GOM_TRA_1PNPDE20050905_194857_000000362040_00300_18390_0003.N1	DC map used
GOM_TRA_1PNPDE20050905_200016_000000372040_00300_18390_0004.N1	DC map used
GOM_TRA_1PNPDE20050905_200214_000000352040_00300_18390_0005.N1	DC map used
GOM_TRA_1PNPDE20050905_200325_000000352040_00300_18390_0006.N1	DC map used
GOM_TRA_1PNPDE20050912_022158_000000372040_00390_18480_0000.N1	DC map with no T dep.
GOM_TRA_1PNPDE20050912_022732_000000392040_00390_18480_0001.N1	DC map used
GOM_TRA_1PNPDE20050912_023115_000000422040_00390_18480_0002.N1	DC map used
GOM_TRA_1PNPDE20050912_023402_000000372040_00390_18480_0003.N1	DC map used
GOM_TRA_1PNPDE20050912_023959_000000432040_00390_18480_0004.N1	DC map used
GOM_TRA_1PNPDE20050912_024303_000000362040_00390_18480_0005.N1	DC map used
GOM_TRA_1PNPDE20050912_024715_000000382040_00390_18480_0006.N1	DC map used
GOM_TRA_1PNPDE20050912_025426_000000372040_00390_18480_0007.N1	DC map used
GOM_TRA_1PNPDE20050912_205409_000000452040_00401_18491_0000.N1	DC map with no T dep.
GOM_TRA_1PNPDE20050912_205752_000000372040_00401_18491_0001.N1	DC map used
GOM_TRA_1PNPDE20050912_210039_000000372040_00401_18491_0002.N1	DC map used
GOM_TRA_1PNPDE20050912_210636_000000382040_00401_18491_0003.N1	DC map used
GOM_TRA_1PNPDE20050912_210941_000000362040_00401_18491_0004.N1	DC map used
GOM_TRA_1PNPDE20050912_211352_000000362040_00401_18491_0005.N1	DC map used
GOM_TRA_1PNPDE20050912_212104_000000372040_00401_18491_0006.N1	DC map used
GOM_TRA_1PNPDE20050915_000138_000000362040_00431_18521_0003.N1	DC map used
GOM_TRA_1PNPDE20050915_000304_000000352040_00431_18521_0004.N1	DC map used
GOM_TRA_1PNPDE20050919_015350_000000382040_00490_18580_0000.N1	DC map with no T dep.
GOM_TRA_1PNPDE20050919_020209_000000382040_00490_18580_0001.N1	DC map used
GOM_TRA_1PNPDE20050919_020739_000000452040_00490_18580_0002.N1	DC map used
GOM_TRA_1PNPDE20050919_021124_000000432040_00490_18580_0003.N1	DC map used
GOM_TRA_1PNPDE20050919_021412_000000372040_00490_18580_0004.N1	DC map used
GOM_TRA_1PNPDE20050919_022009_000000412040_00490_18580_0005.N1	DC map used
GOM_TRA_1PNPDE20050919_022421_000000372040_00490_18580_0006.N1	DC map used
GOM_TRA_1PNPDE20050919_222253_000000022041_00001_18592_0001.N1	DC map used
GOM_TRA_1PNPDE20050926_203108_000000372041_00100_18691_0000.N1	DC map used
GOM_TRA_1PNPDE20050926_203504_000000372041_00100_18691_0001.N1	DC map used
GOM_TRA_1PNPDE20050926_203846_000000372041_00100_18691_0002.N1	DC map used
GOM_TRA_1PNPDE20050926_204847_000000352041_00100_18691_0003.N1	DC map used
GOM_TRA_1PNPDE20050926_205607_000000362041_00100_18691_0004.N1	DC map used
GOM_TRA_1PNPDE20050926_205753_000000372041_00100_18691_0005.N1	DC map used
GOM_TRA_1PNPDE20050928_205512_000000482041_00129_18720_0000.N1	DC map used
GOM_TRA_1PNPDE20050928_205955_000000442041_00129_18720_0001.N1	DC map used
GOM_TRA_1PNPDE20050929_041748_000000322041_00133_18724_0000.N1	DC map used
GOM_TRA_1PNPDE20050929_202340_000000432041_00143_18734_0000.N1	DC map used
GOM_TRA_1PNPDE20050929_202821_000000432041_00143_18734_0001.N1	DC map used
GOM_TRA_1PNPDE20050929_204050_000000372041_00143_18734_0002.N1	DC map used

In fig. 4.5-1 and 4.5-2 it is plotted the average DC inserted by the processor into the level 1b data products for the spectrometers SPA1 and SPB2 (per band: upper, central and lower). From the figures, it can be noted

that the DC is increasing at the expected rate: 400 electrons per year for SPA1 and 500 electrons per year for SPB2.

The same DC values are plotted in fig. 4.5-3 but for some occultations belonging only to the last reporting month.

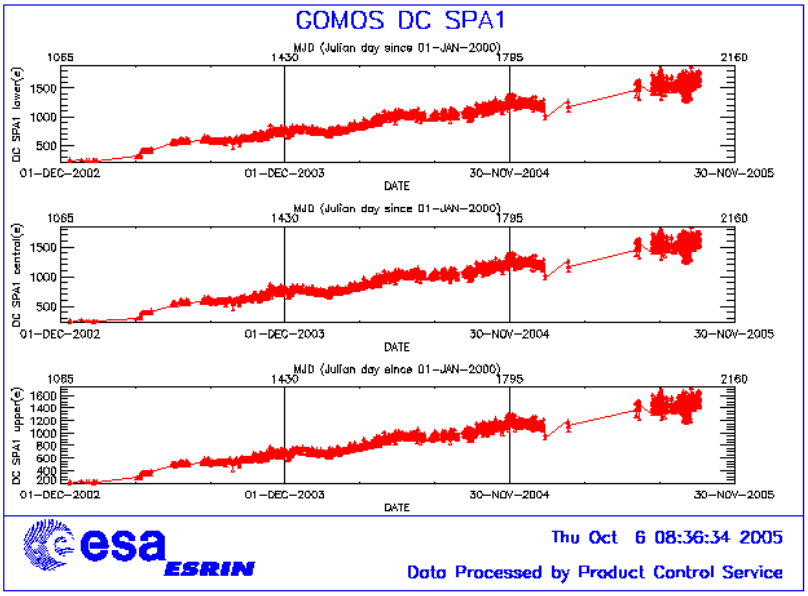

Figure 4.5-1: Mean DC evolution on SPA1 since 15th December 2002 until the end of the reporting period

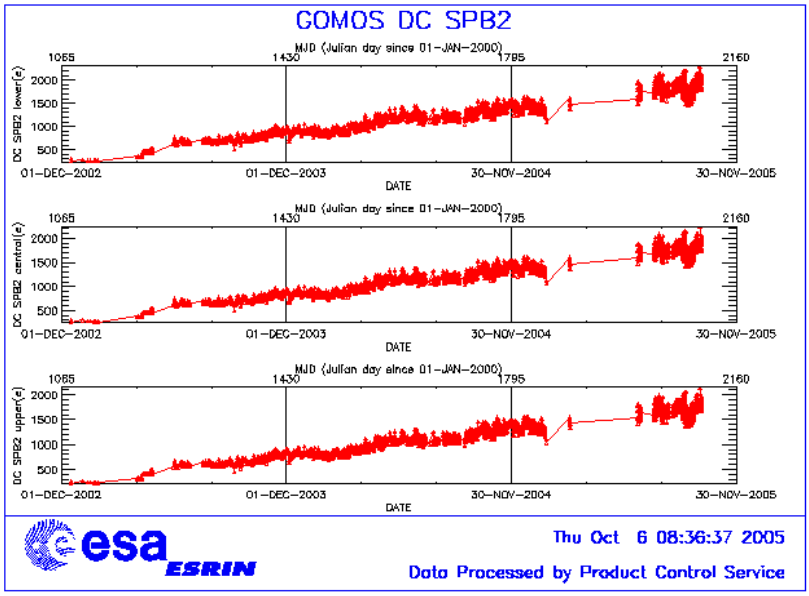

Figure 4.5-2: Mean DC evolution on SPB2 from 15th December 2002 until the end of the reporting period

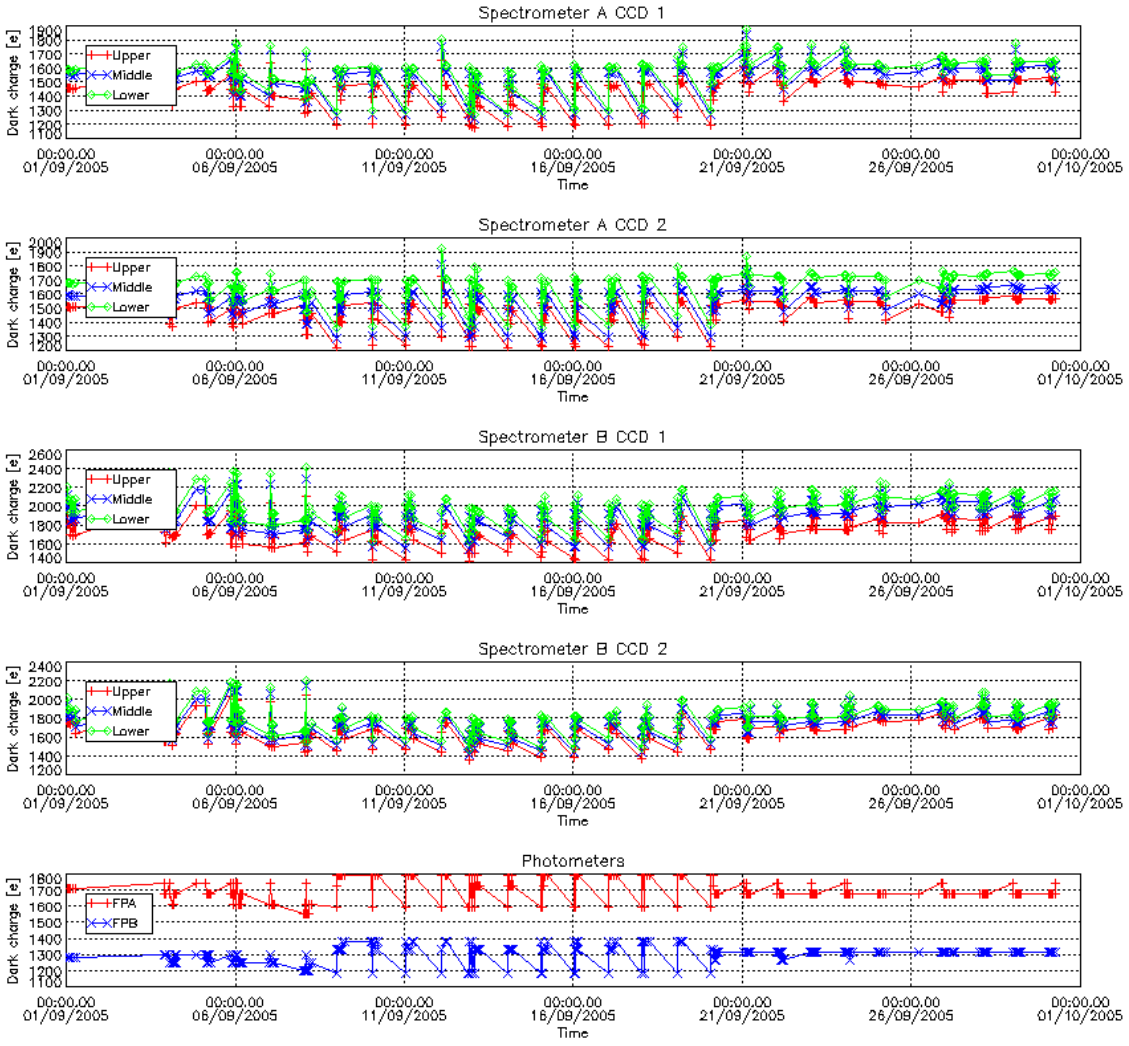

Figure 4.5-3: Mean Dark Charge of spectrometers and photometers during September 2005

4.5.2 SIGNAL MODULATION

A parasitic signal was found to be systematically present, added to the useful signal, at least for spectrometers A1 and A2. The modulation is corrected in the data processing, but the modulation signal standard deviation is routinely monitored in order to detect any trend (fig. 4.5-4).

The modulation standard deviation, for every spectrometer, is characterised as follows:

$$\sigma_{mod} = (\text{'static noises'} - \text{'total static variance'})^{1/2} / \text{gain} \qquad \text{(in ADU)}$$

- The 'static noises' are calculated from the DSA observation performed once per orbit
- The 'total static variance' is obtained from ADF data (electronic chain noise, quantization noise).

The standard deviation of the modulation signal (fig. 4.5-4) presents high values during summer time both 2004 and 2005 years for the ESRIN data, being now confirmed that the South Atlantic Anomaly is the cause of these unexpected peaks. The quality of ESRIN data, in particular over the SAA zone, is thus under investigation. However, in the second half of October 2004 the peaks are smaller because the DSA zone where the data are taking for this analysis is moving towards the Northern Hemisphere. At the end of October 2004 the DSA zone is definitely chosen by the planning system in the Northern Hemisphere (to fill the criteria 'DSA in full dark limb conditions') and the high peaks disappear.

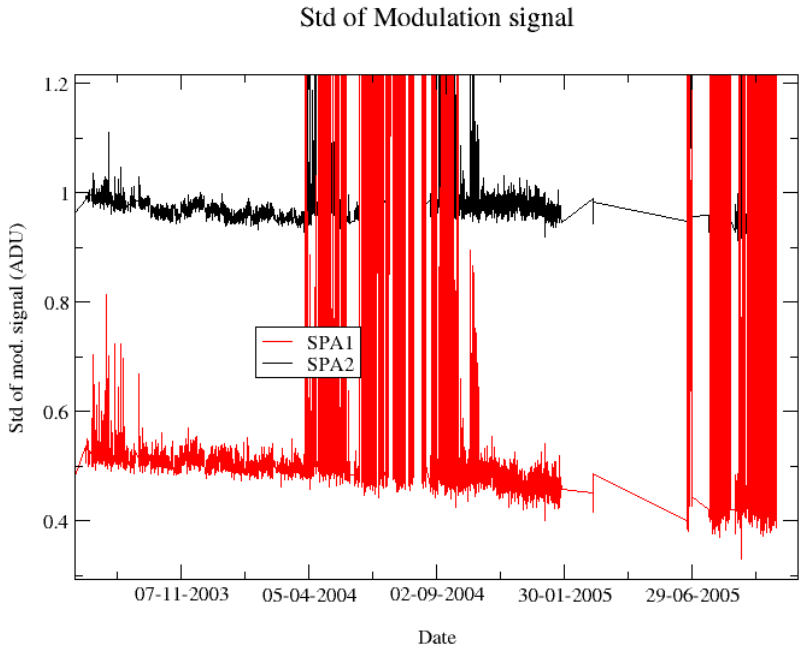

Figure 4.5-4: Standard deviation of the modulation signal

4.5.3 ELECTRONIC CHAIN GAIN AND OFFSET

No new electronic chain gain and offset calibration has been done during the reporting period so these results have been already presented in previous MR.

The routine monitoring of the ADC offset is a good indicator of the ageing of the instrument electronics. During the definition of this routine activity, an exercise has been done to analyze the variation of the ADC offset using the calibration observation in linearity mode (orbits 2810, 4384, 4834, 5219 and 5734).
The fig. 4.5-5 presents the evolution of the calibrated ADC offset for each spectrometer electronic chain. The unexpected increase of this offset seems to be due to an external contribution. In the ADC offset calibration procedure, linearity observations are used with two integration times of 0.25 and 0.50 seconds to extrapolate to an integration time of 0 seconds that give the complete chain offset and not only the ADC offset. The complete offset contains any possible offsets, and especially the static dark charge (i.e. the dark charge that does not depend on the spectrometer integration time). If the memory area of the CCD is affected by the generation of hot pixels (this is confirmed by the presence of vertical lines visible in the

measurement maps in spatial spread monitoring mode), it becomes that the increase observed in fig. 4.5-5 is due to these new hot pixels.

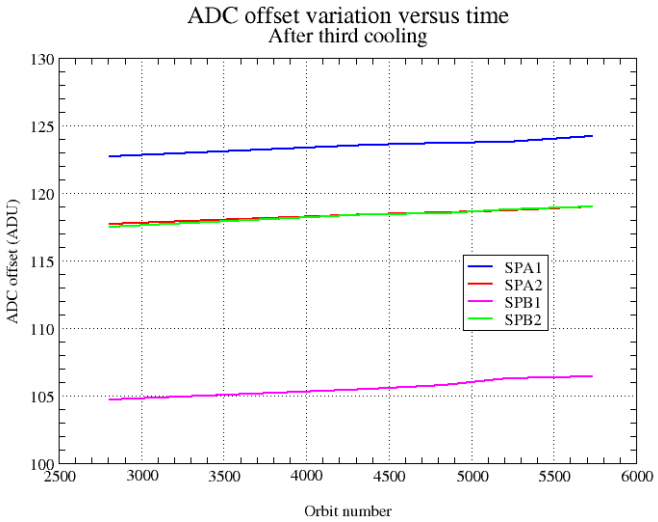

Figure 4.5-5: Evolution of the ADC offset for each spectrometer electronic chain

Next task consists in completing the analysis to confirm that the offset increase is due to the hot pixels in memory area. This can be proven by the study of the noise due to the increased dark charge. The increase of ADC offset will be assumed to be equal to the increase of 'static dark charge' and the corresponding noise will be computed and compared to the increase of the signal variance residual.

If we keep the ADC offset constant, as it is also used to compute the dark charge at band level used to correct the samples in the level 1b processing, the increase of the static dark charge - not taken into account in the ADC offset - is compensated by an artificial increase of the calibrated dark charge. So, the star and limb spectra are correctly corrected for dark charge. A small bias can be added to the instrument noise due to the incorrect dark charge level. Anyway, this quantity is not large enough to require a modification of the ADC offset value.

4.6 Acquisition, Detection and Pointing Performance

4.6.1 SATU NOISE EQUIVALENT ANGLE

The Star Acquisition and Tracking Unit (SATU) noise equivalent angle (SATU NEA) consists of the statistical angular variation of the SATU data above the atmosphere.
The mean of the standard deviation (STD over the 50 values per measurement) above 105 km are computed for every occultation, giving two values per occultation: one in the 'X' direction, one in the 'Y' direction. A mean value per day in every direction and limb is calculated and monitored in order to assess instrument performance in terms of star pointing. The thresholds are 2 and 3 micro radians in 'X' and 'Y' directions respectively. Before May 2003, data above 90 km have been considered (instead of 105 km) but from May

2003 on, data taken in the mesospheric oxygen layer (located around 100 km altitude) have been avoided because they could cause fluctuations on the SATU data. Also the products with errors (error flag set) are discarded from May 2003 onwards.

As it can be seen in fig. 4-6.1, the SATU NEA had a sudden increase on 8th September 2005 due to an unknown reason. It is still well below the threshold but the cause of this unexpected behavior is under investigation.

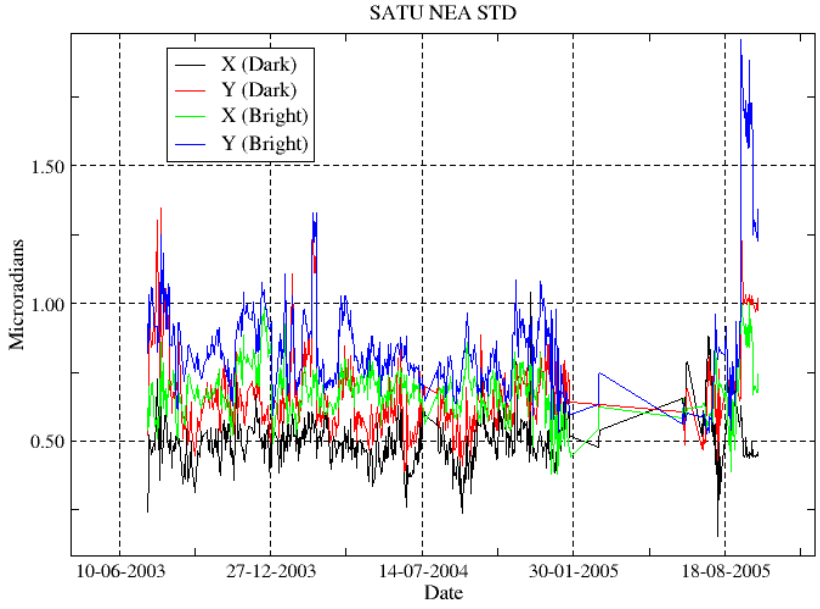

Figure 4.6-1: Average value per day of SATU NEA STD above 105 km

The results for some occultations belonging to previous months (monthly averages) are presented in fig. 4.6-2, where the change in trend in September, mainly for the 'Y' axis is visible.

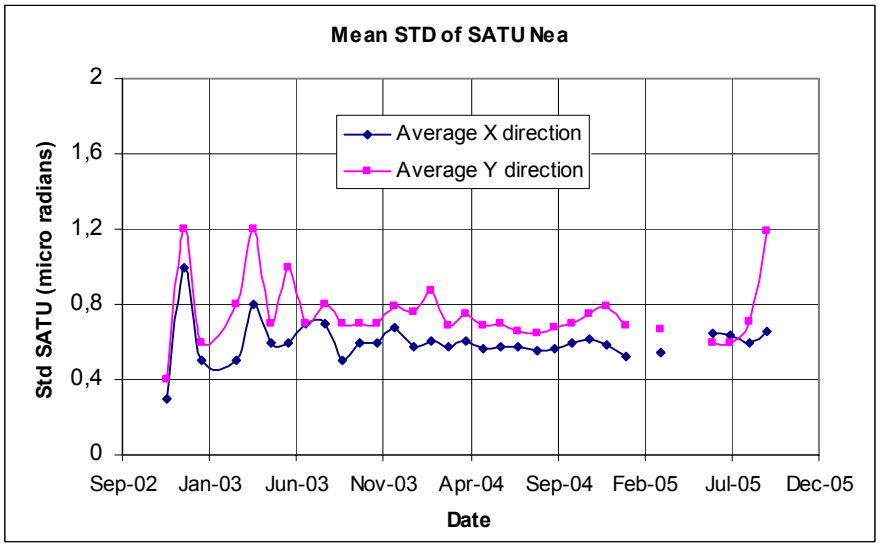

Figure 4.6-2: Average value per month of SATU NEA STD above 105 km

4.6.2 TRACKING LOSS INFORMATION

This verification consists of the monitoring of the tangent altitude at which the star is lost. It is an indicator of the pointing performance although it is to be considered that star tracking is also lost due to the presence of clouds and hence not only due to deficiencies in the pointing performance. Therefore, only the detection of any systematic long-term trend is the main purpose of this monitoring. The recent results are presented in fig. 4.6-3 and 4.6-4:

- The dependence of the altitude at which tracking is lost on the magnitude of the star is very small because the tracking is mainly lost due to the refraction and the scintillation that depend on the atmospheric conditions.
- There is one star lost at very high altitude in dark limb (fig. 4.6-3). It is a "short occultation", that is, occultations planned to have a duration very small (2, 6, 10…seconds) because the azimuth of those stars is very near to the new reduced instrument azimuth edges. To avoid planning that kind of useless occultations, it has been decided to set the minimum occultation duration value to 25 seconds.
- In bright limb, it is not expected that the occultations are lost at a very low altitudes due to the amount of light arriving to the pointing system mainly when the refraction effects start to be important. We see from fig. 4.6-4 that there are stars lost at altitudes around 4 km. This occurs when the pointing system is not able to point to the star anymore but, instead of finishing the occultation, it continues to track light until the planned duration is reached.
- Some daily statistics are given in fig. 4.6-5 (calculated using 50 products per day). The high peaks before the unavailability of GOMOS (25th January 2005) are due to the long lasting occultations or partial occultations. The ones during June/July/August 2005 are due to the tests performed for the anomaly investigation.
- Some monthly statistics are given in fig. 4.6-6 (calculated using 50 products per day) where the change in trends, mainly for dark limb, is visible for the period of GOMOS testing.

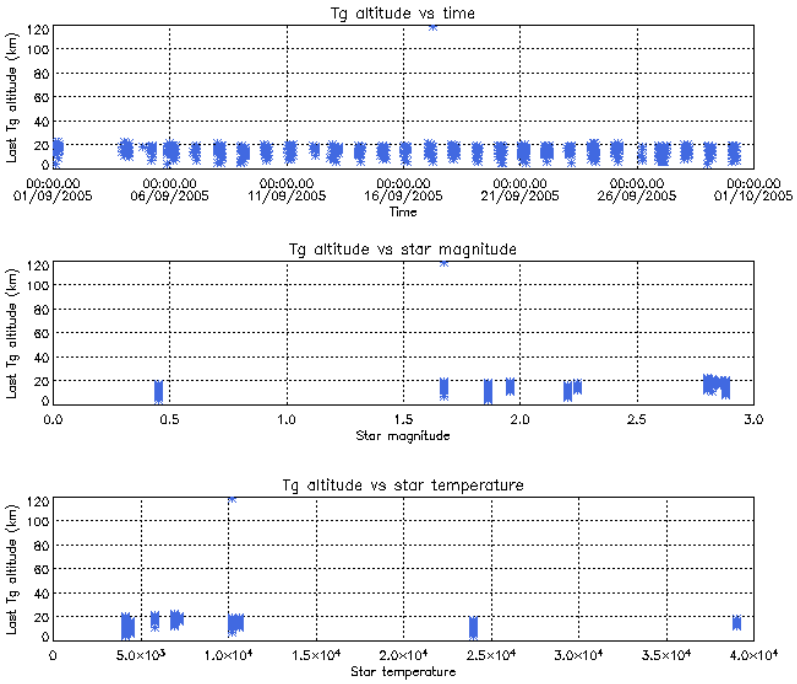

Figure 4.6-3: Last tangent altitude of the occultation (dark limb), point at which the star is lost

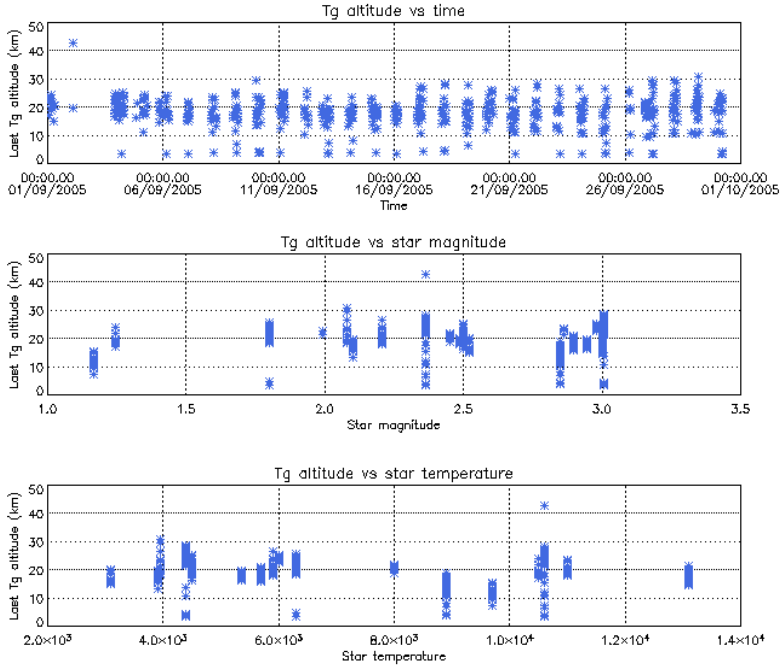

Figure 4.6-4: Last tangent altitude of the occultation (bright limb), point at which the star is lost

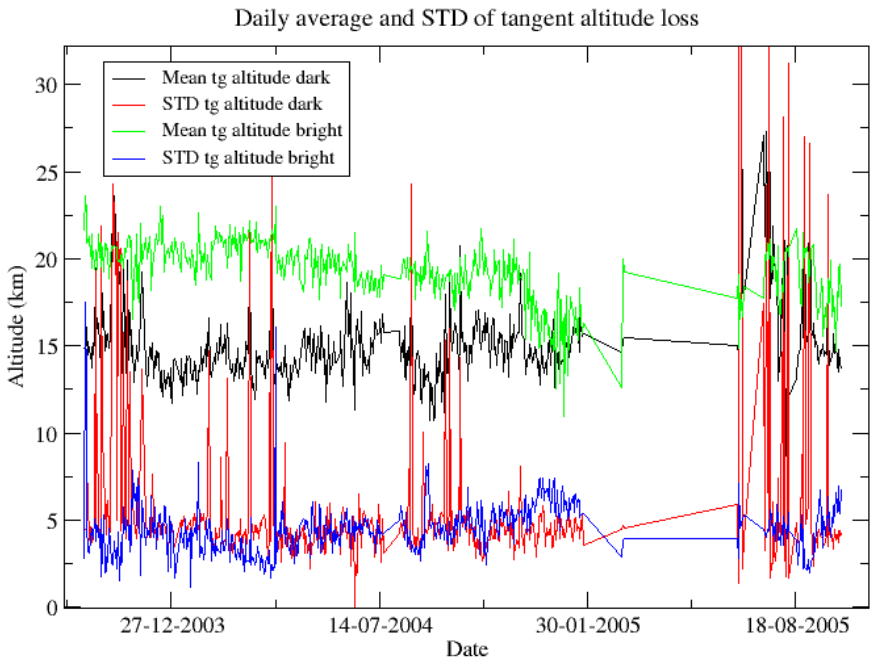

Figure 4.6-5: Daily average and STD of tangent altitude loss for the reporting period

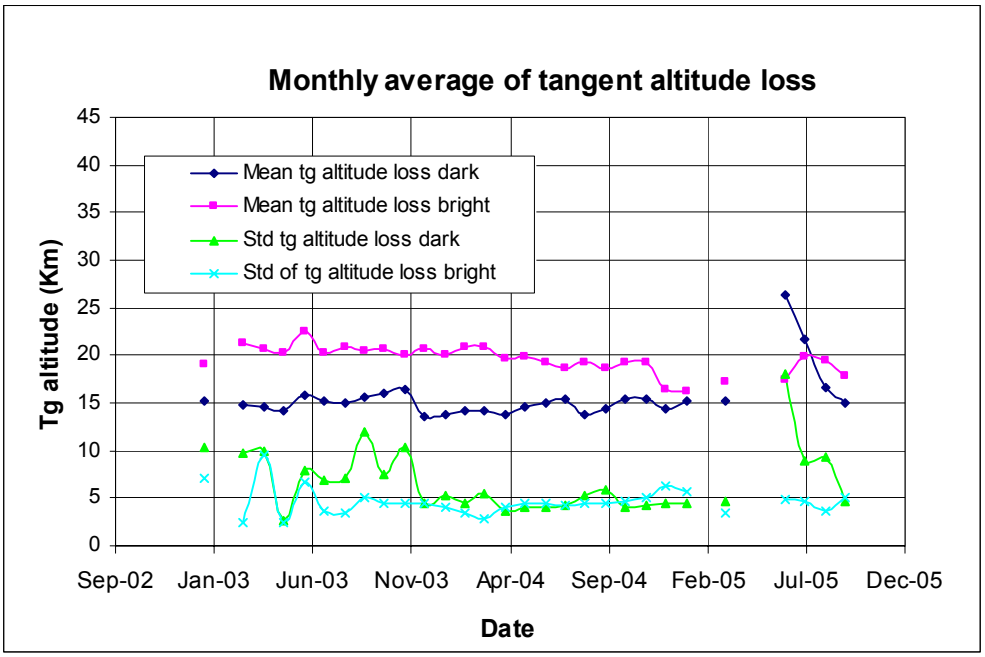

Figure 4.6-6: Monthly mean tangent altitude (and STD) at which the star is lost since January 2003

4.6.3 MOST ILLUMINATED PIXEL (MIP)

The MIP (Most Illuminated Pixel) is the star position on the SATU CCD in detection mode and it is recorded in the housekeeping data. The nominal centre of the SATU is pixel number **145** in elevation and number **205** in azimuth. The detection of the stars should not be far from this centre. As it can be seen in fig. 4.6-7 the **azimuth MIP** was within the threshold (table 4.6-1) since September 2002 until the occurrence of the anomaly on January 2005, even if a small variation is present. The reason for the change in trend observed after the anomaly is, at the moment, not understood. The **elevation MIP** had a significant variation (see the *note* below) until 12th December 2003 when a new PSO algorithm was activated in order to reduce the deviations of the ENVISAT platform attitude with respect to the nominal one. Similarly to the azimuth, after the anomaly of January 2005 the Elevation MIP has a drift that has no explanation. Investigations are on going to try to understand this behavior of the MIP that although does not impact the data quality, it may invalidate attitude monitoring by GOMOS and could represent a hidden anomaly.

Note: A MIP variation onto the SATU CCD of 50 pixels corresponds to a de-pointing of 0.1 degrees

Table 4.6-1: MIP Thresholds

MIP X	**Mean delta Az**	[198 - 210]
	Std delta Az	7
MIP Y	**Mean delta El**	[140 – 150]
	Std delta El	4

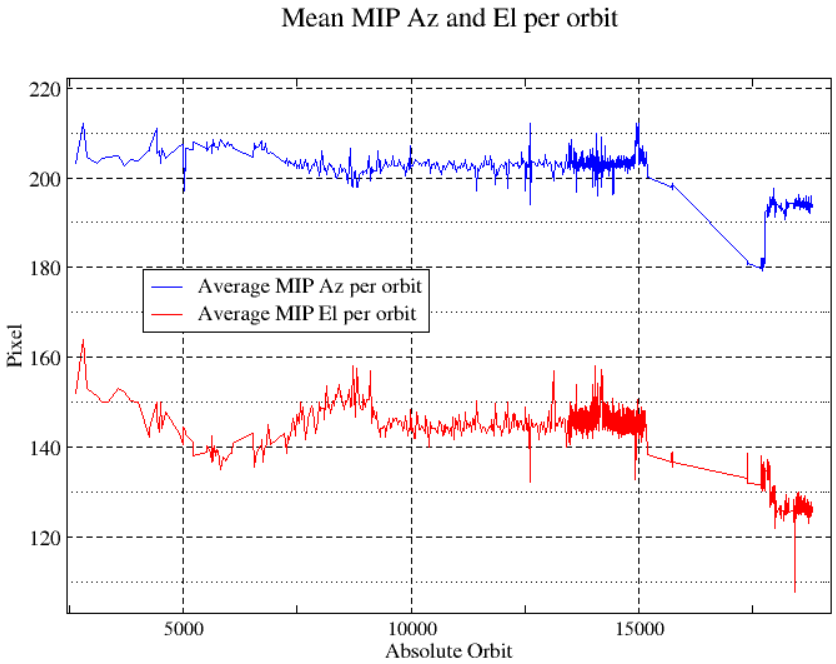

Figure 4.6-7: Mean values of MIP for some orbits since 1st September 2002 (see table 4.6-1)

Fig. 4.6-8 shows the standard deviation of azimuth and elevation MIP that should be within the thresholds of table 4.6-1. The peaks observed mean that one (or more) star/s where detected very far from the SATU

detection point and, in this case, the star/s is lost during the centering phase (see section 3.2 for stars lost in centering).

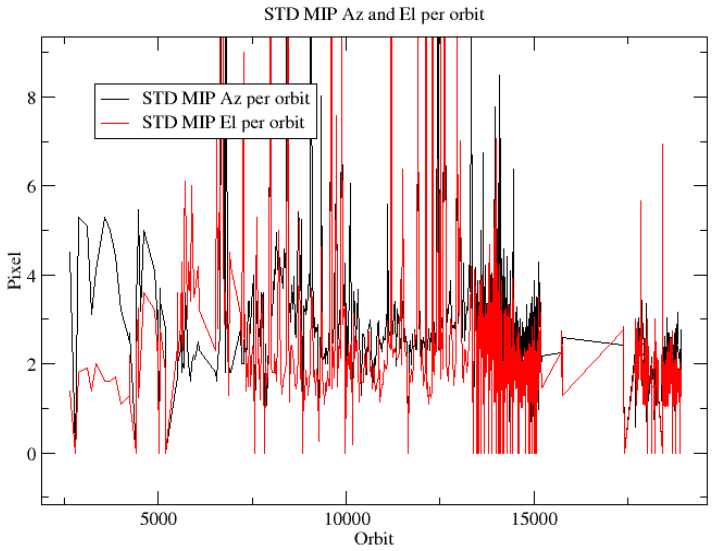

Figure 4.6-8: Standard deviation of MIP Azimuth and Elevation for some orbits since 1st September 2002 until end of reporting period (see table 4.6-1)

5 LEVEL 1 PRODUCT QUALITY MONITORING

5.1 Processor Configuration

5.1.1 VERSION

About 25% of near real time GOM_TRA_1P products have been received by the DPQC team for routine quality control and long term trend quality monitoring. The current level 1-processor software version for the operational ground segment is GOMOS/4.02 (see table 5.1-1). The product specification is PO-RS-MDA-GS2009_10_3H. This processor has been cleared for initial level 1 data release, with a disclaimer for known artefacts (http://envisat.esa.int/dataproducts/availability/disclaimers) that are currently being resolved and will be implemented in the next release (http://envisat.esa.int/dataproducts/availability).

Users are supplied with 2003 data sets reprocessed by the prototype processor GOPR_6.0a developed and operated by ACRI. See table 5.1-2 for prototype level 1b versions and modifications. The version for the second reprocessing (already on-going) is GOPR_6.0c and the next GOMOS operational ground segment version (GOMOS/5.00) will be in line with it.

Table 5.1-1: PDS level 1b product version and main modifications implemented

Date	Version	Description of changes
23-MAR-2004	Level 1b version 4.02 at PDHS-E and PDHS-K	Algorithm baseline level 1b DPM 6.0 • Adding a new calibration parameters (these values are hard

		coded at the moment) • Removal of redundancy chain from code • Modifications in the processing to apply new configuration and calibration parameter • New algorithm to determine between dark, twilight and bright limb and to handle data accordingly • Added handling of source packages with invalid packet header • Added enumerations for all configuration flags • See ref. [2] for more details
31-MAY-2003	Level 1b version 4.00 at PDHS-E and PDHS-K	Algorithm baseline level 1b DPM 5.4: • Modulation correction step added after the cosmic rays detection processing • Inversion of the non-linearity and offset corrections • Modification of the computation of the estimated background signal measured by the photometers: use the spectrometer radiometric sensitivity curve and the photometer transfer function. • Use of the dark charge map at orbit level computed from the DSA (dark sky area) if any in the level 0 product • Implementation of a new unfolding algorithm for the photometer samples • See ref. [2] for more details
21-NOV-2002	Level 1b version 3.61 at PDHS-E and PDHS-K	Algorithm baseline DPM 5.3: • Review of some default values • New definition of one PCD flag (atmosphere) • Temporal interpolation of ECMWF data • See ref. [2] for more details

Table 5.1-2: GOPR level 1b product version and main modifications implemented

Date	Version	Description of changes
22-JUL-2005	GOPR_6.0c	Level 1b: • Correction of FP unfolding algorithm • Background correction of SPB in full dark limb • Modification of the computation of the incidence angle • Correction of the flat-field correction equations • Star spectrum location on CCD modified for SPB Configuration for second reprocessing: • Use of new reflectivity LUT • New wavelength assignment for SPA1, A2, B1 • Spatial PSF of SPB modified
17-MAR-2004	GOPR 6.0a	• Provide SFA and SATU angles in degrees • Elevation angle dependency of the reflectivity LUT added in the algorithms • Ratio upper/star signal added (FLAGUC) • Add Dark Charge used for dark charge correction (per band) • Flag for illumination condition (PCDillum) • Minimum sample value for which the cosmic rays detection processing is applied (Crmin) is a function of gain index • Logic for computation of the flags attached to the reference star spectrum

		(Flref) modified • Add the computation of the sun direction in the inertial geocentric frame to be written in the level 1b and limb products. • Spectrometer effective sampling time added
25-JUL-2003	GOPR 5.4f	• The demodulation process is applied only in full dark limb and twilight limb conditions.
17-JUL-2003	GOPR 5.4e	• Sun zenith angle is computed in the geolocation process. The occultation is now classified into (0) full dark limb condition, (1) bright limb condition and (2) twilight limb condition. • No background correction applied in full dark limb condition. The location of the image of the star spectrum on the CCD array is no more aligned with the CCD lines.
02-JUL2003	GOPR 5.4d	• The maximum number of measurements is set to 509 (instead of 510) in the GOPR prototype.
17-MAR-2003	GOPR 5.4c	• Modification of the CAL ADFs (update of the limb radiometric LUT). The products are affected only if the limb spectra are converted into physical units • Modifications to allow compatibility with ACRI computational cluster (no modifications of the results) • Modification of the logic to handle dark charge map refresh at orbit level (DSA data is now directly processed by the level 1b processor if available in the level 0 product). No impact on the results
21-FEB-2003	GOPR 5.4b	• DC map values are rounded when written in the level 1b product • Modification of the CAL ADFs (update of the wavelength assignment of SPB1 and SPB2) • Modify the computation of flag_mod in the modulation correction routine
17-JAN-2003	GOPR 5.4a	• use the start and stop dates of the occultation when calling the CFI □nterpol instead of start and stop dates of the level 0 product • modify the ECMWF filename information in the SPH of the level 1b and limb products

5.1.2 AUXILIARY DATA FILES (ADF)

The ADF's files in tables 5.1-3, 5.1-4, 5.1-5, 5.1-6 and 5.1-7 have been disseminated to the PDS during the whole mission. Note that the files outlined in yellow are the set of auxiliary files used during the reporting period. For every type of file, the validity runs from the start validity time until the start validity time of the following one, but if an ADF file has been disseminated after the start validity time, it is obvious that it will be used by the PDHS-E and PDHS-K PDS only after the dissemination time (this happens the majority of the times). As the other ADF's, the calibration auxiliary file (GOM_CAL_AX) has been updated several times in the past (table 5.1-7) but the difference is that now it is updated in a weekly basis with only new DC maps, and that is why the files used during March – September 2005 are reported in a separate table (table 5.1-8) that changes from report to report.

Table 5.1-3: Table of historic GOM_PR1_AX files used by PDS for level 1b products generation

Used by PDS for Level 1b products generation in period	GOM_PR1_AX (GOMOS processing level 1b configuration file)
01-MAR-2002 → 29-MAR-2002	**GOM_PR1_AXVIEC20020121_165314_20020101_000000_20200101_000000** • Pre-launch configuration

30-MAR-2002 → 14-NOV-2002	**GOM_PR1_AXVIEC20020329_115921_20020324_200000_20100101_000000** • Changed num_grid_upper, thr_conv and max_iter in the atmospheric GADS
Not used	**GOM_PR1_AXVIEC20020729_083756_20020301_000000_20100101_000000** • Cosmic Ray mode + threshold • DC correction based on maps • Non-linearity correction disabled
Not used	**GOM_PR1_AXVIEC20021112_170331_20020301_000000_20100101_000000** • Central background estimation by linear interpolation + associated thresholds
15-NOV-2002 → 26-MAR-2003	**GOM_PR1_AXVIEC20021114_153119_20020324_000000_20100101_000000** • Same content as GOM_PR1_AXVIEC20021112_170331_20020301_000000_20100101_000000 but validity start updated so as to supersede according to the PDS file selection rules GOM_PR1_AXVIEC20020329_115921_20020324_200000_20100101_000000
27-MAR-2003 → 19-MAR-2004	**GOM_PR1_AXVIEC20030326_085805_20020324_200000_20100101_000000** • Same content as GOM_PR1_AXVIEC20021112_170331_20020301_000000_20100101_000000 but validity start updated so as to supersede according to the PDS file selection rules GOM_PR1_AXVIEC20020329_115921_20020324_200000_20100101_000000
20-MAR-2004 → 22-MAR-2004	**GOM_PR1_AXVIEC20040319_134932_20020324_200000_20100101_000000** • Ray tracing parameter changed: convergence criteria set to 0.1 microrad
23-MAR-2004 → 01-APR-2004 *Notes*: • This file was constructed from GOM_PR1_AXVIEC20030326_085805_20020324_200000_20100101_000000 (so without the ray tracing parameter changed) • This file was used by the GOMOS/4.02 processors before the IECF dissemination. The dissemination was done on 25th March 2004	**GOM_PR1_AXVIEC20040316_144850_20020324_200000_20100101_000000** GOM_PR1 ADF for version GOMOS/4.02, changes: • The central band estimation mode • Atmosphere thickness • Altitude discretisation
02-APR-2004	**GOM_PR1_AXVIEC20040401_083133_20020324_200000_20100101_000000** • Ray tracing parameter changed: convergence criteria set to 0.1 microrad

Table 5.1-4: Table of historic GOM_INS_AX files used by PDS for level 1b products generation

Used by PDS for Level 1b products generation in period	GOM_INS_AX (GOMOS instrument characteristics file)
01-MAR-2002 → 29-JUL-2002	**GOM_INS_AXVIEC20020121_165107_20020101_000000_20200101_000000** • Pre-launch configuration
30-JUL-2002 → 12-NOV-2002	**GOM_INS_AXVIEC20020729_083625_20020301_000000_20100101_000000** • Factors for the conversion of the SFA angles from SFM axes to

	GOMOS axes
13-NOV-2002 → 16-JUL-2003	**GOM_INS_AXVIEC20021112_170146_20020301_000000_20100101_000000** • No more invalid spectral range
Not used	**GOM_INS_AXVIEC20030716_080112_20030711_120000_20100101_000000** • New value for SFM elevation zero offset for redundant chain: 10004
17-JUL-2003	**GOM_INS_AXVIEC20030716_105425_20030716_120000_20100101_000000** • Bias induct azimuth redundant value set to -0.0084 rad (-0.4813 deg)

Table 5.1-5: Table of historic GOM_CAT_AX files used by PDS for level 1b products generation

Used by PDS for Level 1b products generation in period	GOM_CAT_AX (GOMOS Stat Catalogue file)
01-MAR-2002	**GOM_CAT_AXVIEC20020121_161009_20020101_000000_20200101_000000** • Pre-launch configuration

Table 5.1-6: Table of historic GOM_STS_AX files used by PDS for level 1b products generation

Used by PDS for Level 1b products generation in period	GOM_STS_AX (GOMOS Star Spectra file)
01-MAR-2002	**GOM_STS_AXVIEC20020121_165822_20020101_000000_20200101_000000** • Pre-launch configuration

Table 5.1-7: Table of historic GOM_CAL_AX files used by PDS for level 1b products generation

Used by PDS for Level 1b products generation in period	GOM_CAL_AX (GOMOS Calibration file)
01-MAR-2002 → 29-JUL-2002	**GOM_CAL_AXVIEC20020121_164808_20020101_000000_20200101_000000** • Pre-launch configuration
Not used	**GOM_CAL_AXVIEC20020121_142519_20020101_000000_20200101_000000** • Pre-launch configuration
30-JUL-2002 → 12-NOV-2002	**GOM_CAL_AXVIEC20020729_082426_20020717_193500_20100101_000000** • Band setting information • Wavelength assignment • Spectral dispersion LUT • ADC offset for Spectrometers • PRNU maps • Thermistor coding LUT • DC maps
Not used	**GOM_CAL_AXVIEC20021112_165603_20020914_000000_20100101_000000** • Band setting information • DC maps • PRNU maps • Wavelength assignment • Spectral dispersion LUT • Radiometric sensitivity LUT (star and limb) • SP-FP intercalibration LUT • Vignetting LUT

	• Reflectivity LUT • ADC offset
13-NOV-2002 → 30-JAN-2003	**GOM_CAL_AXVIEC20021112_165948_20021019_000000_20100101_000000** • Only DC maps updated
31-JAN-2003 → 11-APR-2003	**GOM_CAL_AXVIEC20030130_133032_20030101_000000_20100101_000000** • Only DC maps updated (using DSA of orbit 04541)
12-APR-2003 → 02-JUN-2003	**GOM_CAL_AXVIEC20030411_065739_20030407_000000_20100101_000000** • Modification of the radiometric sensitivity curve for the limb spectra. Note that the modification of this LUT has no impact on the GOMOS processing. The LUT is just copied into the level 1b limb product for user conversion purpose. • Updated DC map only (using DSA of orbit 05762).
03-JUN-2003: from this date onwards, mainly updates to DC maps are done. Every month, the table of new GOM_CAL files with **only** DC maps updated is provided (table 5.1-8). Eventual changes to this file not corresponding only to DC maps updates will be reported in this table.	**GOM_CAL_AXVIEC20030602_094748_20030531_000000_20100101_000000** • Updated DC maps only (using DSA of orbit 06530)
13-FEB-2004 → 23-FEB-2004	**GOM_CAL_AXVIEC20040212_103916_20040209_000000_20100101_000000** • Update of the reflectivity LUT • Updated DC maps (Orbit 10194, date 11-FEB-2004)

Table 5.1-8: Calibration ADF for reporting period. These files are updated (only with DC maps) in a 8-10 days basis

Used by PDS for Level 1b products generation in period	GOM_CAL_AX (GOMOS Calibration file)
05-MAR-2005 → 27-JUN-2005	**GOM_CAL_AXVIEC20050304_134628_20050302_000000_20100101_000000** (orbit 15730, date 04 MAR 2005)
28-JUN-2005 → 03-AUG-2005	**GOM_CAL_AXVIEC20050627_100506_20050626_000000_20100101_000000** (orbit 17345, date 24 JUN 2005)
04-AUG-2005 → 12-AUG-2005	**GOM_CAL_AXVIEC20050803_124403_20050801_000000_20100101_000000** (orbit 17903, date 02 AUG 2005)
13-AUG-2005 → 25-AUG-2005	**GOM_CAL_AXVIEC20050812_135656_20050810_000000_20100101_000000** (orbit 18029, date 11 AUG 2005)
26-AUG-2005 → 02-SEP-2005	**GOM_CAL_AXVIEC20050825_110110_20050824_000000_20100101_000000** (orbit 18211, date 24 AUG 2005)
03-SEP-2005 → 08-SEP-2005	**GOM_CAL_AXVIEC20050902_124352_20050831_000000_20100101_000000** (orbit 18317, date 31 AUG 2005)
09-SEP-2005 → 19-SEP-2005	**GOM_CAL_AXVIEC20050908_122716_20050907_000000_20100101_000000** (orbit 18416, date 07 SEP 2005)
20-SEP-2005 → 07-OCT-2005	**GOM_CAL_AXVIEC20050919_104724_20050917_000000_20100101_000000** (orbit 18576, date 18 SEP 2005)

5.2 *Quality Flags Monitoring*

In this section it is monitored some Product Quality information stored in level 1b products that did not have a fatal error (MPH error flag not set). The products with fatal errors were around 1% of the products received during March – September 2005 for the quality monitoring.

On the one hand, for every product we have information of the **number of measurements** where a given problem was detected (i.e. number of invalid measurements, number of measurements containing saturated samples, number of measurements with demodulation flag set…). On the other hand, there are **flags** that indicate problems within the product (i.e. flag set to one if the reference spectrum was computed from DB, flag set to zero if SATU data were not used…).

For the information on the number of measurements a plot of percentages with respect to time is provided in fig. 5.2-1. Part of this information, the most relevant one, is also plotted in a world map as a function of ENVISAT position: % of cosmic ray hits per profile, % of datation errors per profile, % of star falling outside the central band per profile and % of saturation errors per profile (fig.5-2.2).

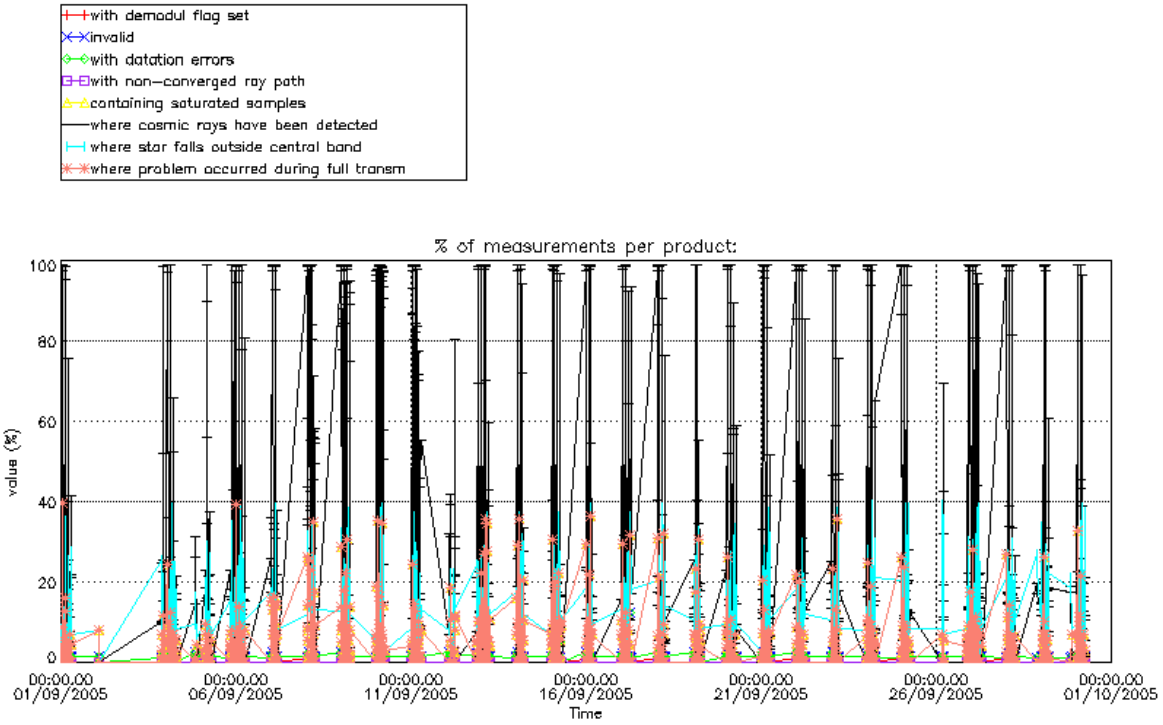

Figure 5.2-1: Level 1b product quality monitoring with respect to time

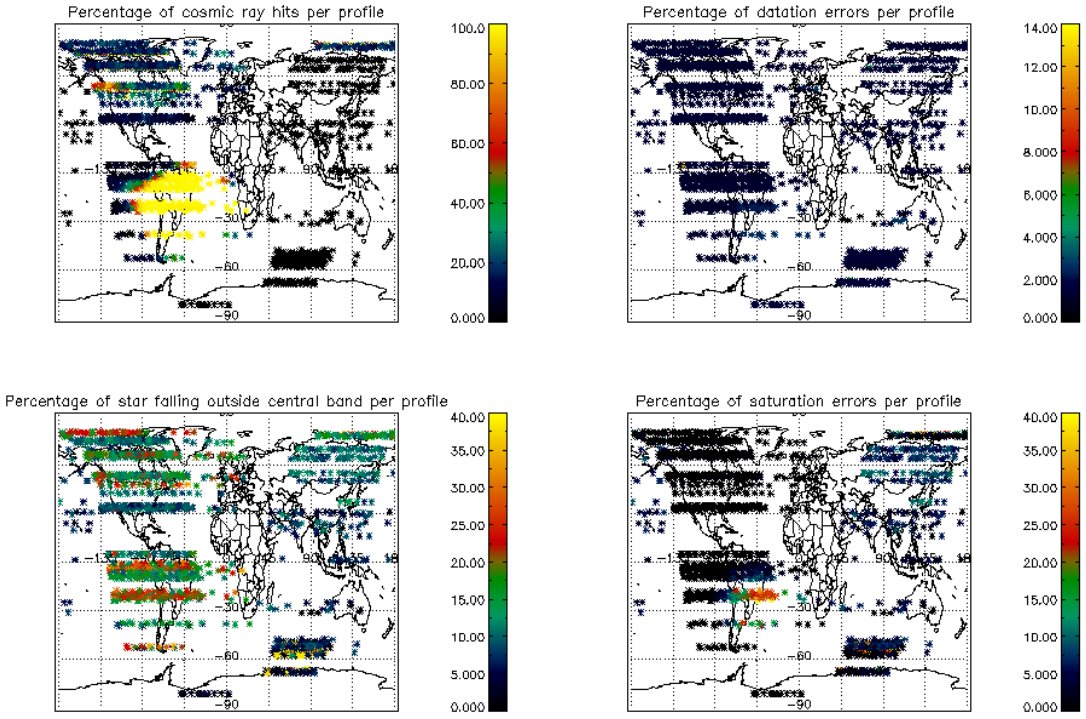

Figure 5.2-2: Level 1b product quality monitoring with respect to geolocation of ENVISAT

It can be seen from fig. 5.2-1 that the cosmic rays hits occurred several times for the 95% of the measurements of the products. Looking at fig. 5.2-2 it can be clearly observed that this high percentage occurred when the satellite crossed the South Atlantic Anomaly (SAA) zone. Also the percentage of saturation errors per profile increased over SAA zone.
Another observation from fig. 5.2-1 is that, for many products, the 25 % of the measurements have the star signal falling outside the central band. In fig. 5.2-2 it is observed that this percentage occurred mainly during the ascending part of the orbit (night-side of the orbit) while in the descending part (day-side of the orbit) the percentage is around 10 %. This is because during the night the stars are lost deeper within the atmosphere and the turbulence phenomena become more important, producing the star to be less 'focused' on the spectrometers central band.
The other values (% of invalid measurements per product, % of measurements per product with datation errors…) are quite low.

The flag information is given in table 5.2-1. It is reported also the percentage of the products that have at least one measurement with demodulation flag set.

Table 5.2-1: Percentage of products during the reporting period with:

At least one measurement with demodulation flag set:	20.6051 %
Reference spectrum computed from DB:	0.00000 %
Reference spectrum with small number of measurements:	0.00000 %
SATU data not used:	0.00000 %

5.2.1 QUALITY FLAGS MONITORING (EXTRACTED FROM LEVEL 2 PRODUCTS)

In this section it is plotted the Product Quality information coming from the level 1 processing but stored also in the level 2 products. Only products that did not have a fatal error (MPH error flag not set) are considered. The purpose of using the level 2 data is simply that the percentage of level 2 products arriving to the DPQC team for the quality monitoring is much higher. For September, 65% of the archived products have been received. The plots are very similar to fig. 5.2-1 and 5.2-2 (demodulation flag information is not included) but separating ascending from descending passes. The ascending part of the orbit is in dark limb while the descending is in bright limb. In ascending, twilight occultations are located in the South Pole while in descending they are located in the North Pole.

Fig. 5.2-3 and 5.2-4 present some quality information as a function of the time whereas in fig. 5.2-5 and 5.2-6 the plot is respect to the satellite position at the beginning of the occultations. In ascending (fig. 5.2-5) the SAA is perfectly localized by the high percentage of cosmic ray hits per product (upper left panel). It is not the same if we look fig. 5.2-6, because in descending the most of the occultations are in bright limb conditions and the cosmic rays detection processing is not activated.

Another clear difference between ascending and descending is that in ascending (fig. 5.2-3) the percentage of measurements "where a problem occurred during the full transmission" per product is around 2% while for the descending passes is around 10%. This is due to the saturation that occurs mainly in bright limb. In ascending the saturation occurs over the SAA zone but it is quite low elsewhere. The high percentage of cosmic ray hits per product (yellow peaks) in fig. 5.2-4 is due to a very intense solar activity occurred on 8th September that sparked a strong radiation storm over the poles.

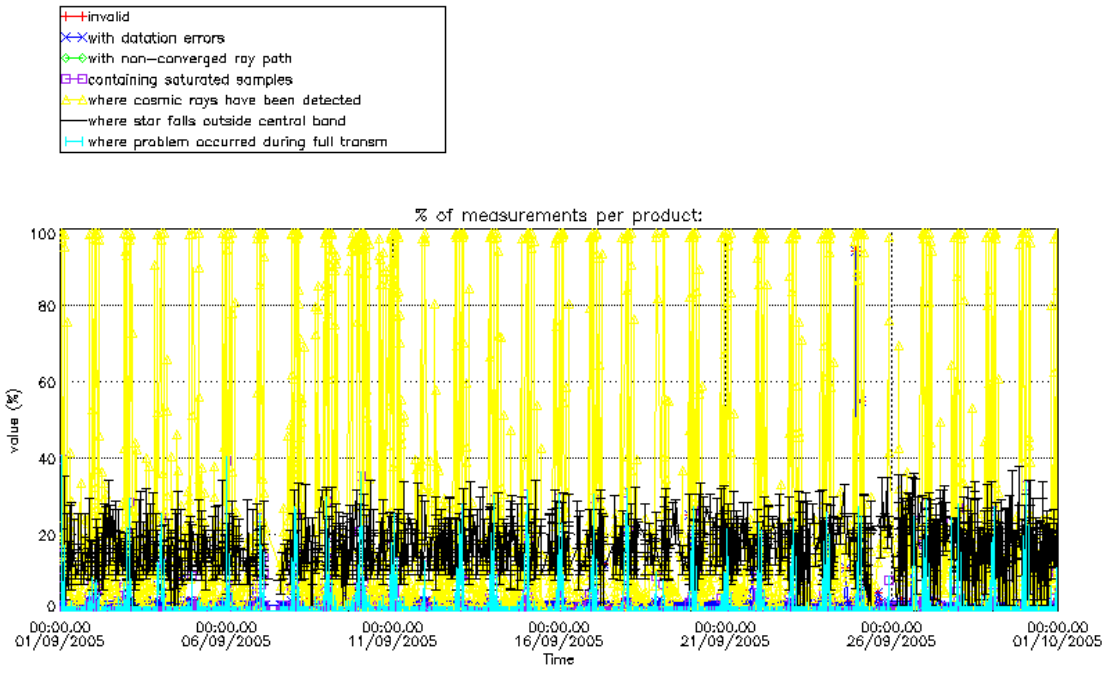

Figure 5.2-3: Level 1b product quality monitoring with respect to time ASCENDING ENVISAT passes

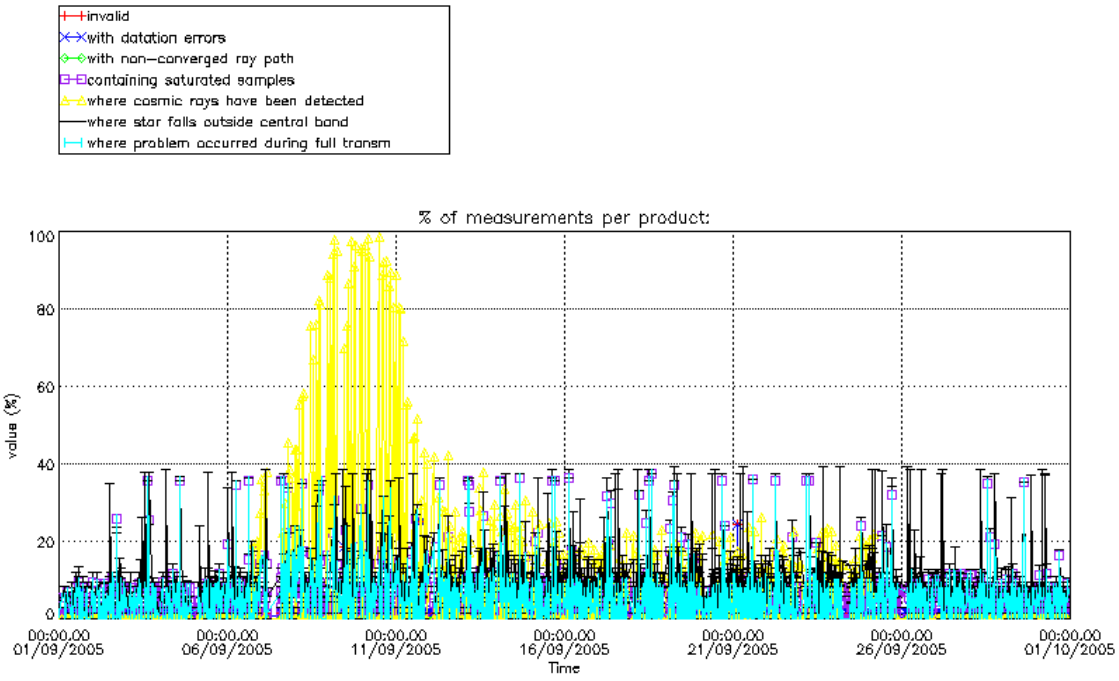

Figure 5.2-4: Level 1b product quality monitoring with respect to time <u>DESCENDING</u> ENVISAT passes

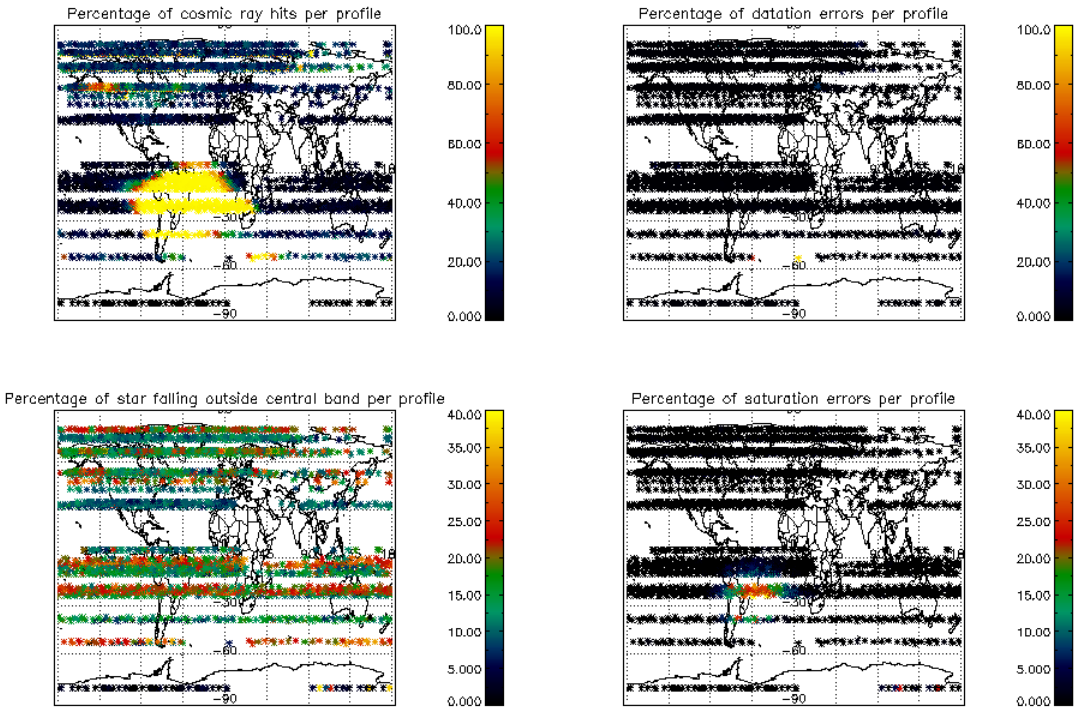

Figure 5.2-5: Level 1b product quality monitoring with respect to geolocation for <u>ASCENDING</u> ENVISAT passes

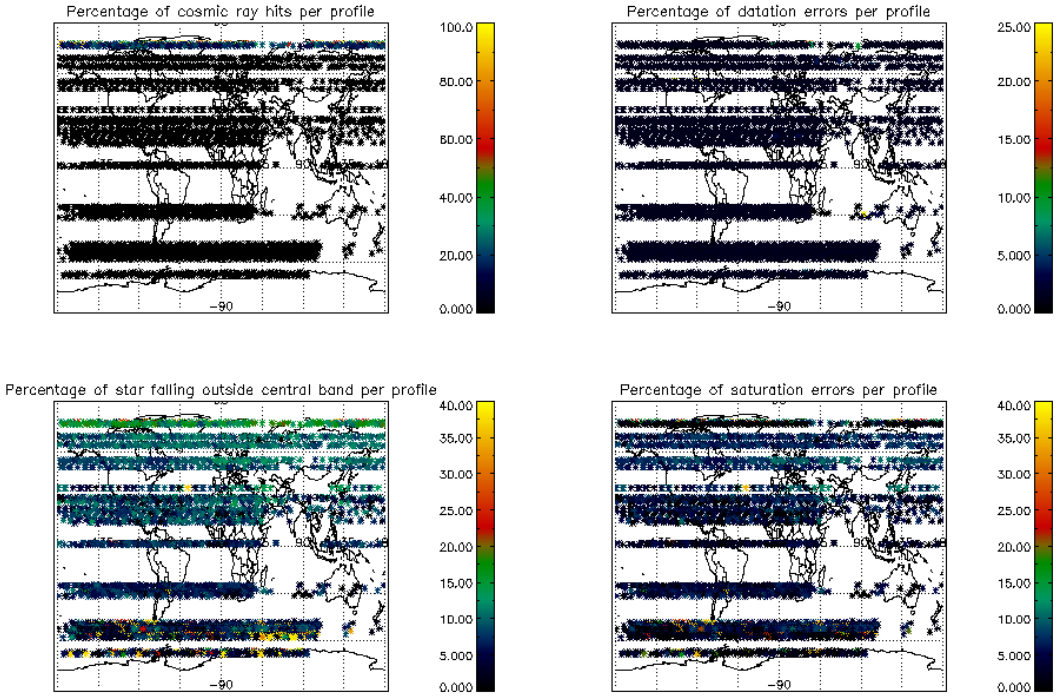

Figure 5.2-6: Level 1b product quality monitoring with respect to geolocation for DESCENDING ENVISAT passes

5.3 Spectral Performance

A new spectral calibration has been performed during the reporting period. As occurred during previous calibrations, the results exceed the warning values.

The values reported in the plot of fig. 5.3-1 are, for every star ID (1, 2, 4, 9, 18, 25), the spectral shift on SPA2 CCD for which a maximum correlation has been found between the reference spectrum and the one of the occultation.

During the last wavelength calibration analysis performed using two occultations on 28th September 2005, the spectral shifts were greater than 0.07 (warning value) and QWG has decided to recalibrate the wavelength assignment when the new processor will be ready.

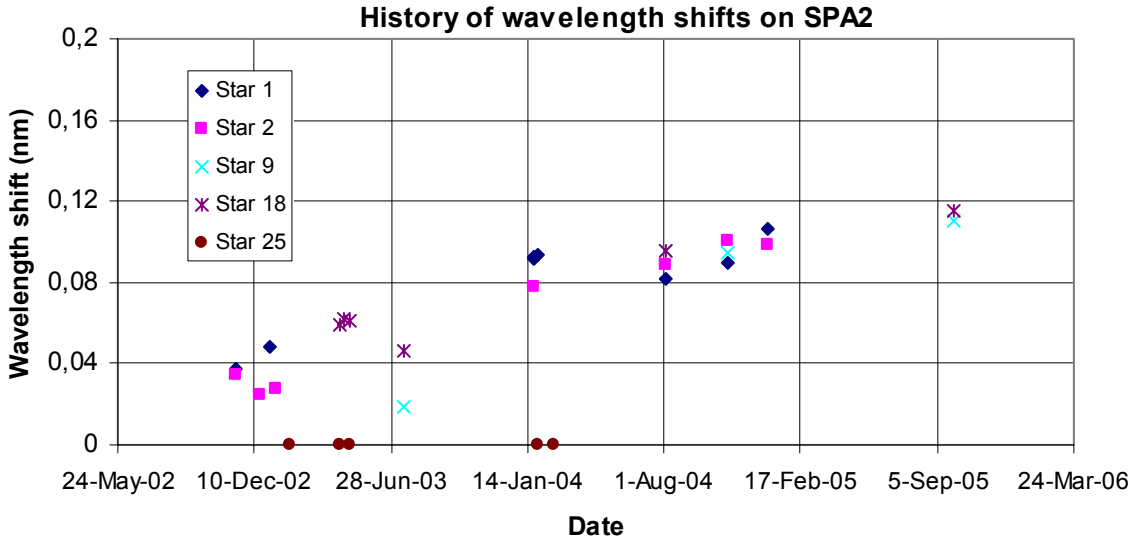

Figure 5.3-1: Wavelength shifts on SPA2 since 12th November 2002 calculated using different stars

5.4 Radiometric Performance

5.4.1 RADIOMETRIC SENSITIVITY

The monitoring performed consists in the calculation of the radiometric sensitivity of each CCD by computing the ratio between parts of the reference spectrum using specific stars. The parts of spectrum used are:

- UV: 250–300 nm
- Yellow: 500–550 nm
- Red: 640–690 nm
- Ir1: 761-770 nm
- Ir2: 935-944 nm

For the spectrometers the ratios are with respect to the 'yellow' spectral range. For the photometers, the ratio is calculated dividing the mean photometer signal above the atmosphere (115 km) by the 'yellow' spectral range (for PH1) or by the 'red' spectral range (for PH2).

The variation of the ratio should be within a given threshold actually set to 10% (see table 5.4-1 that corresponds to fig. 5.4-1). For every star, this variation is calculated as the difference between the maximum (or minimum) ratio, and the mean over the 15 first values (if there were not 15 values computed yet, all values would be used).

Table 5.4-1: Variation of RS for the different ratios (corresponds to fig. 5.4-1). Should be less than 10%

Star Id	% Variation of UV ratio	% Variation of Red ratio	% Variation of IR1 ratio	% Variation of IR2 ratio	% Variation of Ph1 ratio	% Variation of Ph2 ratio
1	2.44196	0.545067	0.401701	0.250543	8.55029	30.1656
2	0.641065	0.705293	0.625175	0.383392	8.27717	7.93166
4	0.150048	0.844181	1.52463	1.30163	8.08780	23.5227
9	12.4407	0.989038	0.783493	0.466555	5.59734	9.05862
18	1.73015	0.919592	0.844914	0.852089	14.7885	299.989
25	19.2603	0.715622	1.04061	1.12662	28.0870	147.396

For star 25 and 9 the UV ratio is greater than the threshold 10%. It is clear (fig. 5.4-1) that there is a global decrease of UV ratios for all the stars. This confirms the expected degradation suffered by the UV optics that is, anyway, very small considering also the small variation for the rest of the stars (table 5.4-1).

By looking at the photometers radiometric sensitivity ratios of fig. 5.4-1, it can be seen that every star has a variation that seems to be annual. The variation is significant for stars 25 and 18. After some investigations performed by the QWG that exclude an inaccurate reflectivity correction LUT or the different limbs (dark, twilight, bright) as sources of the variation, it has been concluded that the problem is not linked to the photometers. A further indication that the problem is not on the photometer sensitivity is that every star has a very different behaviour.

UV

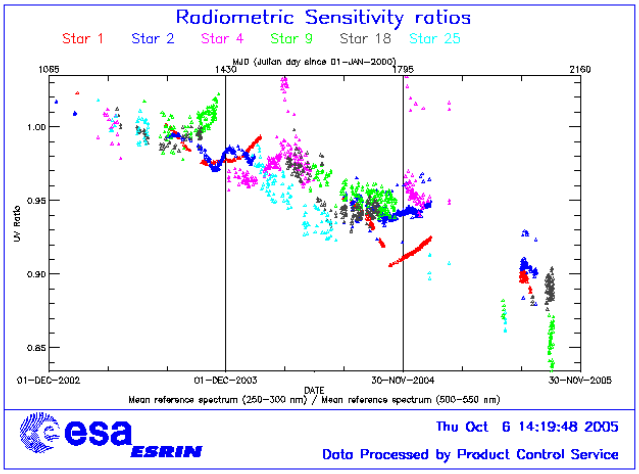

VIS

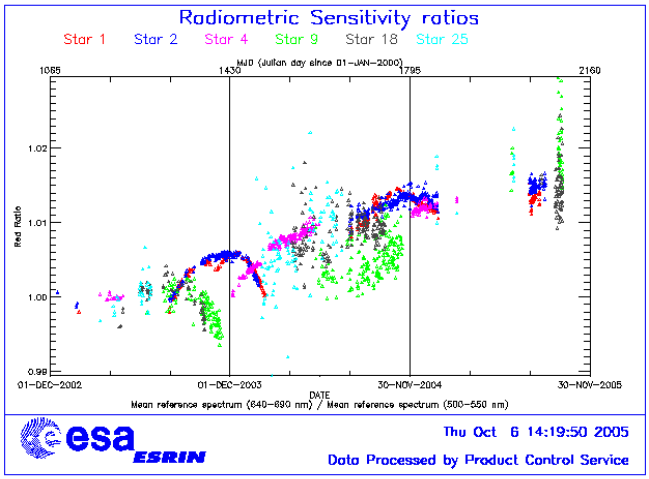

IR1

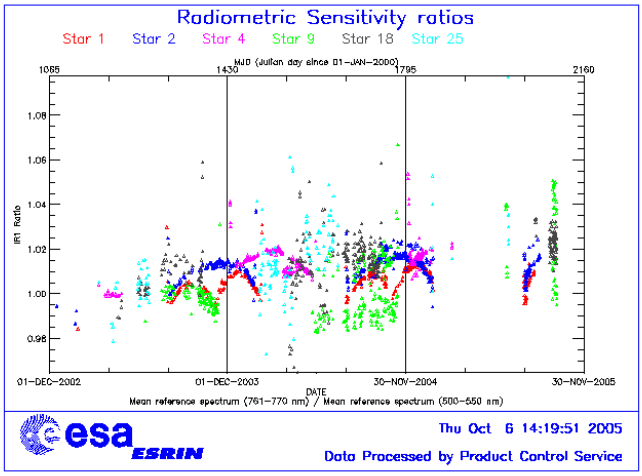

IR2

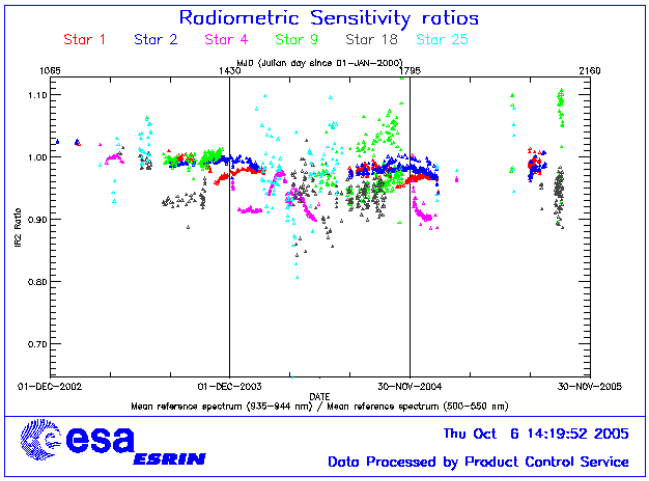

PH1

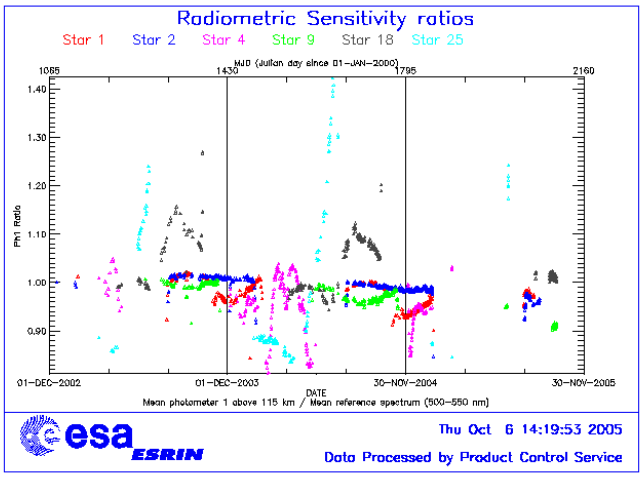

PH2

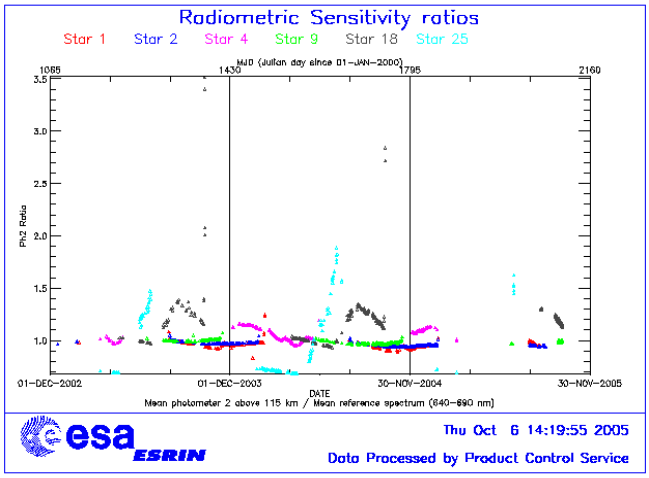

Figure 5.4-1: Radiometric sensitivity ratios since December 2002

5.4.2 PIXEL RESPONSE NON UNIFORMITY

No new PRNU calibration has been performed during the reporting period. This means that the PRNU maps inside the ADF remain as they are without any change for the moment.

5.5 Other Calibration Results

Future reports will address other calibration results, when available.

6 LEVEL 2 PRODUCT QUALITY MONITORING

6.1 Processor Configuration

6.1.1 VERSION

Level 2 products from the operational ground segment have been disseminated during September to the users. About 65% of GOM_NL__2P products have been received by the DPQC team for routine quality control and long term trend monitoring. The current level 2-processor software version for the operational ground segment is GOMOS/4.02 (see table 6.1-1). The product specification is PO-RS-MDA-GS2009_10_3H. The improvements defined at the first Validation Workshop have been implemented into the prototype processor GOPR 6.0a (see table 6.1-2), and the first reprocessing activity (for 2003 data) has been performed with this prototype. A second reprocessing is on-going (for years 2002, 2003 and 2004) with the prototype version GOPR 6.0f (see table 6.1-2). The next operational ground segment processor GOMOS/5.00 will be in line with it.

Table 6.1-1: PDS level 2 product version and main modifications implemented

Date	Version	Description of changes
23-MAR-2003	Level 2 version 4.02 at PDHS-E and PDHS-K	Algorithm baseline level 2 DPM 5.5: Section 3 • Add references to technical notes on Tikhonov regularization • Change High level breakdown of modules: SMO/PFG • Change parameter: NFS in l2 ADF • Change parameter σ_G in l2 ADF (Table 3.4.1.1-II) • Change content of Level 2/res products – GAP • Change time sampling discretisation • Add covariance matrix explanation Section 5 • Replace SMO by PFG VER-1/2: Depending on NFS, Apply either a Gaussian filter or a Tikhonov regularization to the vertical

		inversion matrix • Unit conversion applied on kernel matrix • Suppress VER-3 Section 6 • GOMOS Atmospheric Profile (GAP): not used in this version • Time sampling in equation (6.5.3.7-73) • See ref. [3] for more details
31-MAY-2003	Level 2 version 4.00 at PDHS-E and PDHS-K	Algorithm baseline level 2 DPM 5.4: • Revision of some default values • Add a new parameter • Transmission model computation: suppress tests on valid pixels and species • Apply a Gaussian filter to the vertical inversion matrix • Very low signal values are substituted by threshold value • See ref. [3] for more details
21-NOV-2002	Level 2 version 3.61 at PDHS-E and PDHS-K	Algorithm baseline level 2 DPM 5.3a: • Revision of some default values • Wording of test T11 • Dilution term computation of jend • Covariance computation scaling applied before and after • See ref. [3] for more details

Table 6.1-2: GOPR level 2 product version and main modifications implemented

Date	Version	Description of changes
14-OCT-2005	GOPR_6.0f	• The optimisation of the DOAS iterations • Negative column densities and local densities not flagged anymore • Suppress the setting of maximum error in case of negative local densities • Correction of HRTP discrepancies, and error estimates fixed Configuration for second reprocessing: • 2nd order polynomial for aerosol • Air fixed to ECMWF (local density set to 0 in the L2 products) • Orphal cross-sections for O_3 • GOMOS cross-sections for NO_2 • Covariance matrix terms linked to air set to 0 • Air and NO_2 additional errors set to 0
17-MAR-2004	GOPR 6.0a	• Rename Turbulence MDS into High Resolution Temperature MDS (HRTP) • Add vertical resolution per species in local densities MDS • Add Solar zenith angle at tangent point and at satellite level in geolocation ADS • Add "tangent point density from external model" in geolocation ADS • Suppress contribution of "tangent point density from external model" in "local air density from GOMOS atmospheric profile" in geolocation

		ADS (to be completed)
18-AUG-2003	GOPR 5.4d	• Tikhonov regularisation is implemented
18-MAR-2003	GOPR 5.4b	• Modification to implement the computation of Tmodel for spectrometer B (in version 5.4b, the Tmodel for SPB is still set to 1)
30-JAN-2003	GOPR 5.4a	• Modifications for ACRI internal use only. No impact on level 2 products.

6.1.2 AUXILIARY DATA FILES (ADF)

The ADF's files in table 6.1-3 and 6.1-4 are used by the PDS to process the data from level 1 to level 2. For every type of file, the validity runs from the start validity time until the start validity time of the following one, but if an ADF file has been disseminated after the start validity time, it is obvious that it will be used by the PDHS-E and PDHS-K PDS only after the dissemination time (this happens the majority of the times). Note that the files outlined in yellow are the set of auxiliary files used during the reporting period.

Table 6.1-3: Table of historic GOM_PR2_AX files used by PDS for level 2 products generation

Used by PDS for Level 2 products generation in period	GOM_PR2_AX (GOMOS Processing level 2 configuration file)
01-MAR-2002 → 29-JUL-2002	**GOM_PR2_AXVIEC20020121_165624_20020101_000000_20200101_000000** • Pre-launch configuration
30-JUL-2002 → 02-SEP-2002	**GOM_PR2_AXVIEC20020729_083851_20020301_000000_20100101_000000** • Maximum value of chi2 before a warning flag is raised (set to 5) • Maximum number of iterations for the main loop (set to 1)
03-SEP-2002 → 12-NOV-2003	**GOM_PR2_AXVIEC20020902_151029_20020301_000000_20100101_000000** • Maximum value of chi2 before a warning flag is raised (set to 100)
13-NOV-2003 → 22-MAR-2004	**GOM_PR2_AXVIEC20021112_170458_20020301_000000_20100101_000000** • Smoothing mode • Hanning filter • Number of iterations • Spectral windows to suppress the O2 absorption in the high spectral range of SPA2
23-MAR-2004 *Note*: this file was used by the GOMOS/4.02 processors before the IECF dissemination. The dissemination was done on 25th March 2004	**GOM_PR2_AXVIEC20040316_145613_20020301_000000_20100101_000000** • Pressure at the top of the atmosphere • Number of GOMOS sources data (used in GAP) • Activation flag for GOMOS sources data (GAP) • Smoothing mode (after the spectral inversion) • Atmosphere thickness

Table 6.1-4: Table of historic GOM_CRS_AX files used by PDS for level 2 products generation

Used by PDS for Level 2 products generation in period	GOM_CRS_AX (GOMOS Cross Sections file)
01-MAR-2002 → 08-MAR-2002	**GOM_CRS_AXVIEC20020121_164026_20020101_000000_20200101_000000** • Pre-launch configuration

09-MAR-2003 → 29-JUL-2002	**GOM_CRS_AXVIEC20020308_185417_20020101_000000_20200101_000000** • Corrected NUM_DSD in MPH - was 14 and is now 19 - and corrected spare DSD format by replacing last spare by carriage returns in file GOM_CRS_AXVIEC20020121_164026_20020101_000000_20200101_000000
30-JUL-2002 → 25-MAR-2004	**GOM_CRS_AXVIEC20020729_082931_20020301_000000_20100101_000000** • O3 cross-sections summary description (SPA) • NO3 cross-sections summary description • O2 transmissions summary description • H2O transmissions summary description • O3 cross sections (SPA)
26-MAR-2004 *Note*: the file was disseminated on 27 Jan 2004 but could not be used by PDS until version GOMOS/4.02 was in operation	**GOM_CRS_AXVIEC20040127_150241_20020301_000000_20100101_000000** • Update of the O2 and H2O transmissions (S.A input) • Extension by continuity of the O3 cross-section for SPB

6.1.3 RE-PROCESSING STATUS

For many reasons, not only PDS, but also the status of the Calibration and Validation activities at the end of the commissioning phase and the status of the processors (all these points being linked together), it has been very difficult to distribute good products to the user community. To support the Calibration and Validation activities, some products have been generated using the prototypes and disseminated by the ESL on dedicated platforms. It is important to propose, not only to the Calibration and Validation teams but also to all the user community complete data sets for the period 2002 – 2003 – 2004 of Level 1b and Level 2 products, reprocessed from a completed consolidated Level 0 data set.

6.1.3.1 First reprocessing

Data from the first reprocessing activity covering the year 2003 can be retrieved via web query from http://www.enviport.org/gomos/index.jsp. FTP access to bulk reprocessing results (one tar file of GOMOS products per day) is allowed from the D-PAC: ftp://gomo2usr@ftp-ops.de.envisat.esa.int.

The table 6.1-5 presents the status of the first GOMOS reprocessing task in terms of availability of the instrument, level 0 input products and level 1b/2 output products. The status is presented by cycle. Each cycle is made of 501 orbits or 35 days. The last three columns of the table indicate the percentage of availability of each item with respect to the instrument availability in observation mode (i.e. for example without taking account the calibration or DSA observation of GOMOS).Values greater than 100% may occur due to the fact that some calibration observations are not taken into account in the instrument availability but they can be processed. See more details on http://www.fr-acri.com/gomval_web/news/board.htm

Table 6.1-5: Summary of reprocessing status at ACRI

Cycle	Orbits	Cycle Time Interval	% Instr. Availability	% L0 in ACRI	% Lv1b/L2 in ACRI
5	556-1056	08/04/02 21:59 - 13/05/02 20:18	89.6	0.0	0.0
6	1057-1557	13/05/02 21:59 -17/06/02 20:18	86.4	0.0	0.0
7	1558-2058	17/06/02 21:59 - 22/07/02 20:18	88.8	0.2	0.0
8	2059-2559	22/07/02 21:59 - 26/08/02 20:18	88.0	0.0	0.0
9	2560-3060	26/08/02 21:59 - 30/09/02 20:18	75.0	7.2	0.0
10	3061-3561	30/09/02 21:59 - 04/11/02 20:18	95.4	2.7	0.0
11	3562-4062	04/11/02 21:59 - 09/12/02 20:18	88.4	0.0	0.0
12	4063-4563	09/12/02 21:59 - 13/01/03 20:18	95.0	0.0	0.0
13	4564-5064	13/01/03 21:59 - 17/02/03 20:18	97.4	78.7	78.5
14	5065-5565	17/02/03 21:59 - 24/03/03 20:18	60.7	95.7	95.4
15	5566-6066	24/03/03 21:59 - 28/04/03 20:19	84.6	77.4	75.2
16	6067-6567	28/04/03 21:59 - 02/06/03 20:18	14.0	94.3	94.3
17	6568-7068	02/06/03 21:59 - 07/07/03 20:19	52.9	85.7	84.9
18	7069-7569	07/07/03 21:59 - 11/08/03 20:19	65.1	97.2	97.2
19	7570-8070	11/08/03 21:59 - 15/09/03 20:19	84.0	95.2	94.3
20	8071-8571	15/09/03 21:59 - 20/10/03 20:19	93.6	97.2	96.8
21	8572-9072	20/10/03 21:59 - 24/11/03 20:19	92.6	98.9	98.1
22	9073-9573	24/11/03 21:59 - 29/12/03 20:19	90.6	102.8	102.8
23	9574-10074	29/12/03 21:59 - 02/02/04 20:19	95.0	0.0	0.0
24	10075-10575	02/02/04 21:59 - 08/03/04 20:19	95.2	0.0	0.0
25	10576-11076	08/03/04 21:59 - 12/04/04 20:19	96.6	0.0	0.0
26	11077-11577	12/04/04 21:59 - 17/05/04 20:19	100.0	0.0	0.0
27	11578-12078	17/05/04 21:59 - 21/06/04 20:19	46.3	0.0	0.0
28	12079-12579	21/06/04 21:59 - 26/07/04 20:19	0.0	0.0	0.0
29	12580-13080	26/07/04 21:59 - 30/08/04 20:19	0.0	0.0	0.0

6.1.3.2 Second reprocessing

The second reprocessing activity covering the years 2002, 2003 and 2004 is on-going at will be completed at the end of the year 2005. In order to select the best configuration to be used for this activity, testing datasets have been generated with different configurations of the GOPR prototype. The impact of several parameters: choice of the aerosol model, choice of the database for the cross-sections, air density fixed to ECMWF... has been assessed by the QWG. It is presented here the main results of this study, performed by FMI, SA, BIRA-IASB, RIVM (project EQUAL by Y. Meijer) and by ACRI.

All the prototype versions used for testing have the following baseline configuration:

- DOAS iteration stop based on NO_2 and NO_3 line density values
- Flagging of negative column densities and of negative local densities removed
- Setting to maximum error in case of negative local densities removed
- Discrepancies identified in HRTP corrected

Then, several items may be tuned or modified:

- Aerosol model: $1/\lambda$, first degree polynomial or second degree polynomial
- Bremen cross-section for O_3 and NO_2
- Air density fixed to ECMWF values

The assessment of the results by a specific GOPR version is performed by comparison to another GOPR version considered as a reference version. Only one change of the configuration is assessed at a time:

separate assessment of the impact of the aerosol model and the impact of the choice of the cross-section database for instance.
Testing datasets of several hundreds of occultations in full dark limb have been generated with different configurations, and they are compared between them.

Median profiles and standard deviation (or percentile limits) of the column density or of the local density for a dataset generated with a GOPR version are compared to the same dataset generated by the reference version. Median profiles of χ^2 values and residual values may also be assessed. The statistical comparison of O_3 vertical profiles to external measurements may also highlight important features (systematic differences in specific altitude ranges) for the assessment of the configurations.

6.1.3.2.1 Impact of choosing Orphal (Bremen) database instead of GOMOS database

The use of Bremen cross-sections instead of GOMOS ones yields to a small increase of the median value of the O_3 local densities in the middle stratosphere (results at low latitudes shown on fig. 6.1-1).

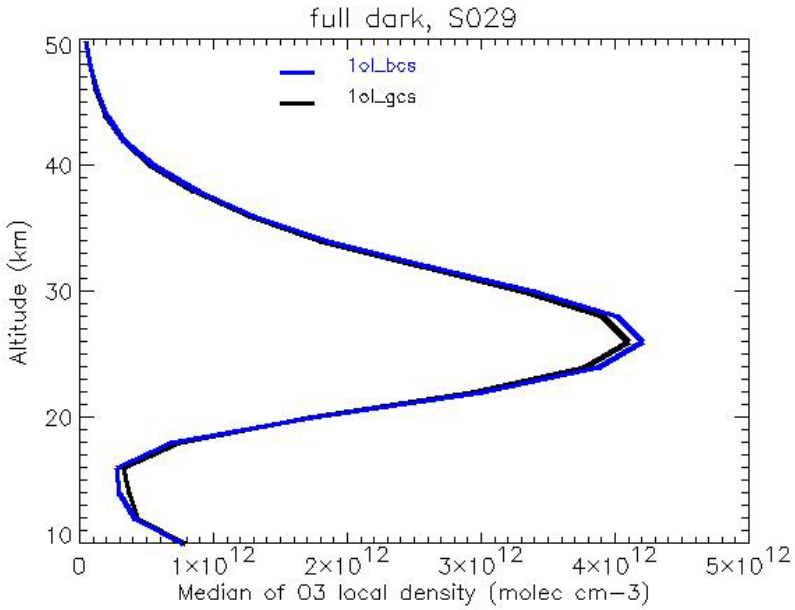

Figure 6.1-1: Vertical profile of the median of O_3 local density (blue: configuration with Bremen cross-sections; black: configuration with GOMOS cross-sections). Results are based on a dataset of 567 dark limb occultations at low latitudes

The relative difference between the median values of the local densities ("Bremen" – reference) shows positive values of a few % between 20km and 50km (fig. 6.1-2).

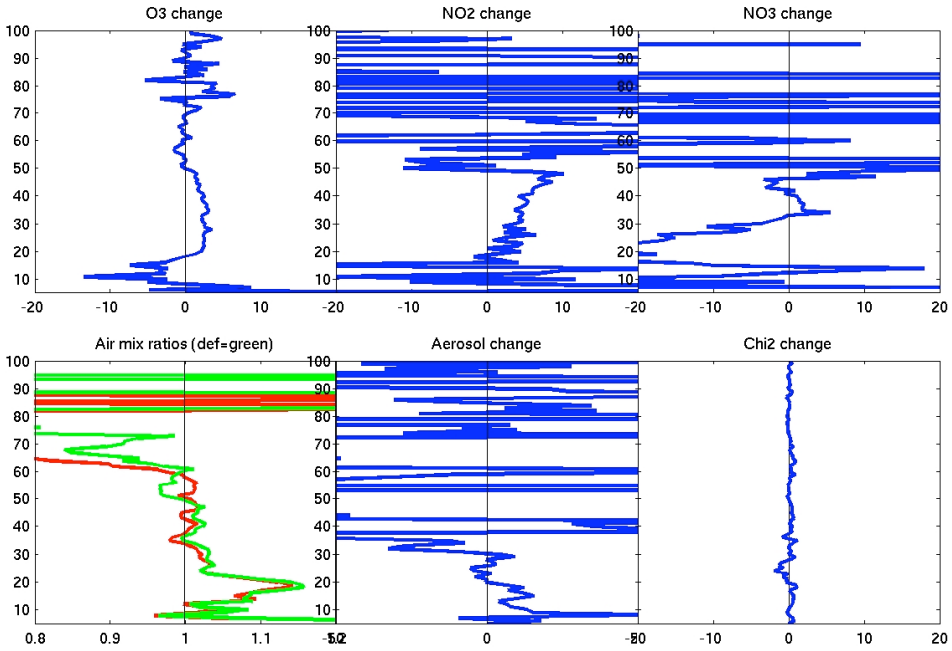

Figure 6.1-2: Comparison between two different configurations: Bremen cross-sections and GOMOS cross-sections (1/λ law for the aerosol model). Results are based on a dataset of 241 dark limb occultations at various latitudes. Top row: Vertical profiles of the relative difference ("Bremen" – "GOMOS") between median of O_3, NO_2, NO_3 local densities by the two configurations. Bottom row: Vertical profiles of the air mixing ratio by the two configurations, of the relative difference between median of the aerosol extinction coefficient, and of the relative difference between the median of the χ^2 values from the two configurations

In general this increase of the O_3 local density with the configuration using Bremen cross-sections improves the comparison with ground-based measurements (decrease of the median of the difference between profiles by the two configurations, especially between 18km and 30km; see results presented on fig. 6.1-3, to be compared to results presented on fig. 6.1-4).

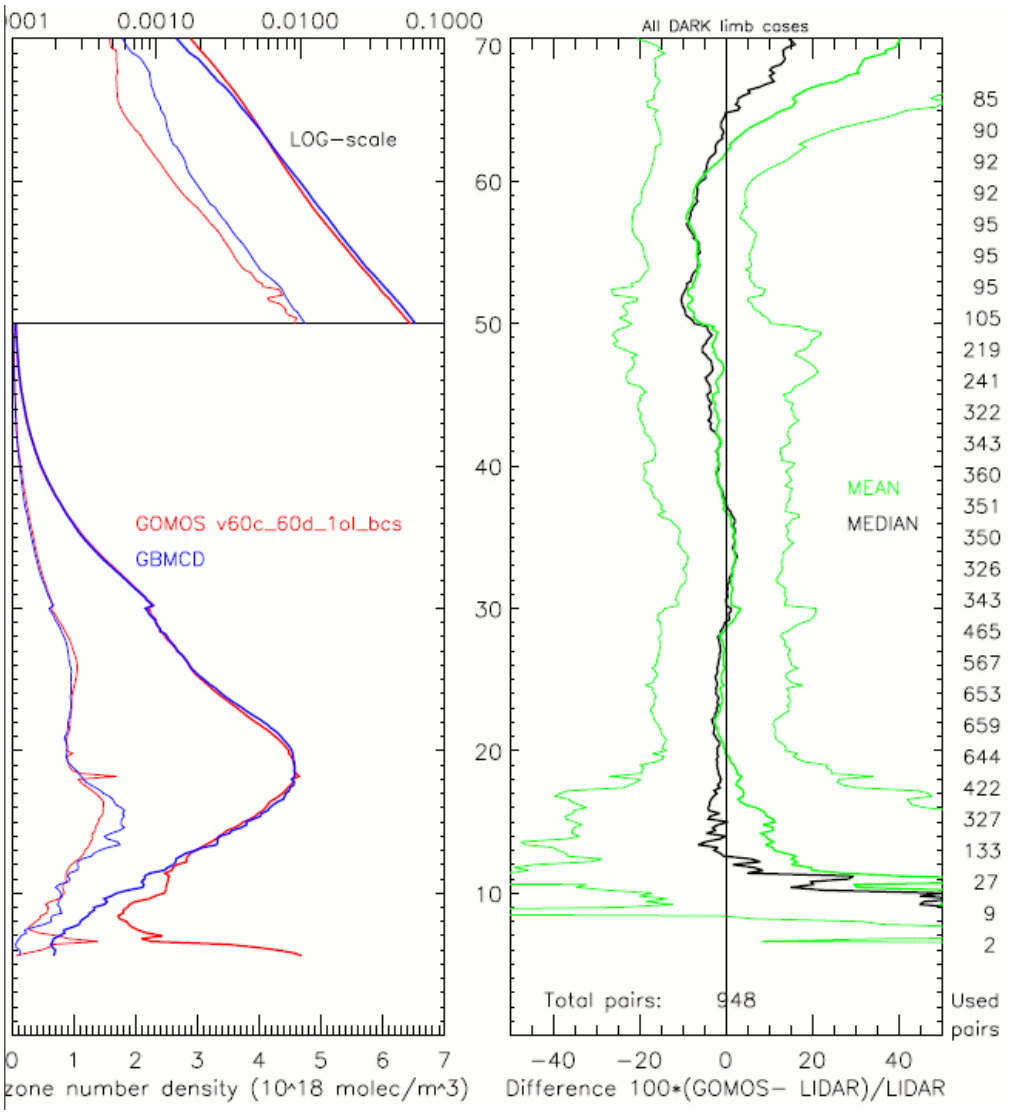

Figure 6.1-3: Vertical profiles of the average and dispersion of GOMOS O_3 local density retrieved with the configuration: Bremen cross-sections and 1/λ law aerosol model (blue line), and measured by ground-based instruments (red line). Top left figure: logarithmic scale between 50km and 70km; bottom left figure: linear scale between 0 and 50km. Vertical profiles of the average relative difference between GOMOS and ground-based measurements of O_3 local density profiles (right figure)

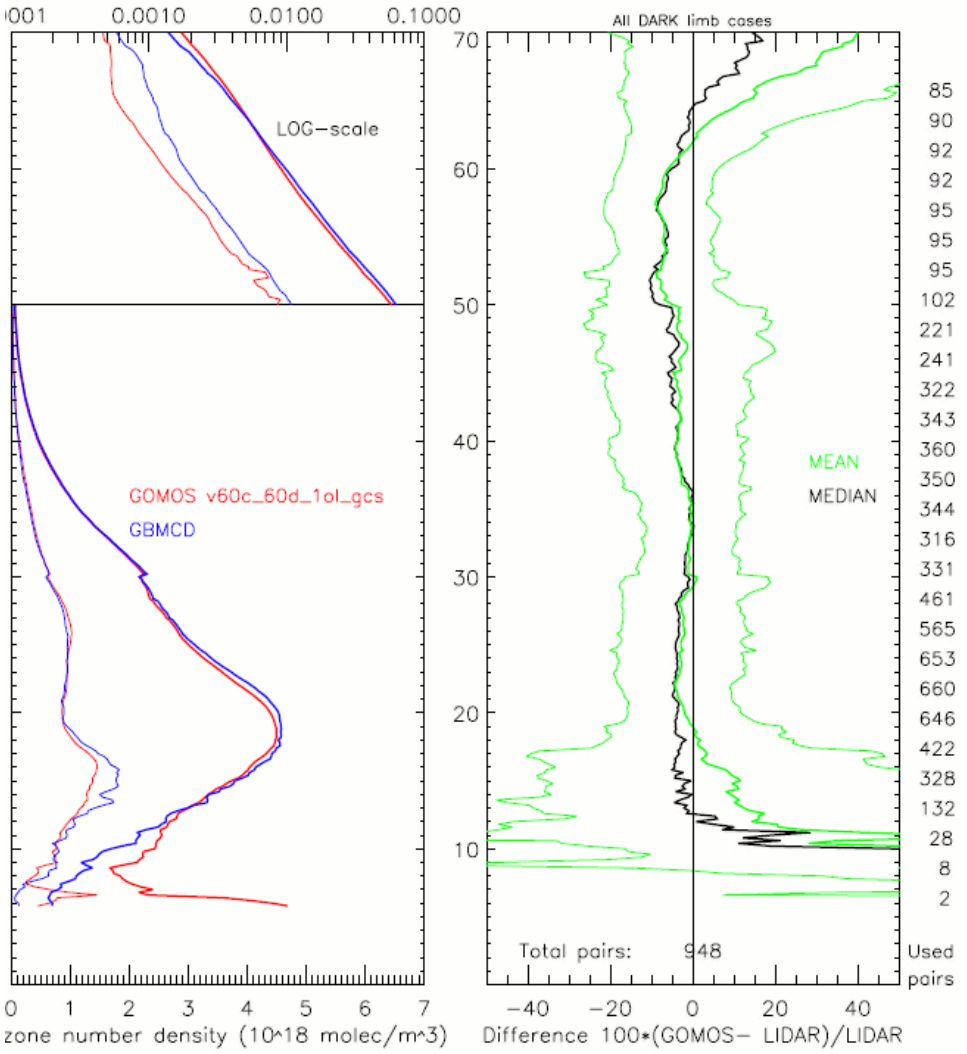

Figure 6.1-4: Vertical profiles of the average and dispersion of GOMOS O_3 local density retrieved with the configuration: GOMOS cross-sections and 1/λ law aerosol model (blue line), and measured by ground-based instruments (red line). Top left figure: logarithmic scale between 50km and 70km; bottom left figure: linear scale between 0 and 50km. Vertical profiles of the average relative difference between GOMOS and ground-based measurements of O_3 local density profiles (right figure)

The NO_2 median value of the local density is also globally increased between 20km and 50km and in a larger extent around 30km-35km (results at low latitudes shown on fig. 6.1-5). Positive values of the relative difference between the median profiles are obtained in this altitude range (fig. 6.1-2).

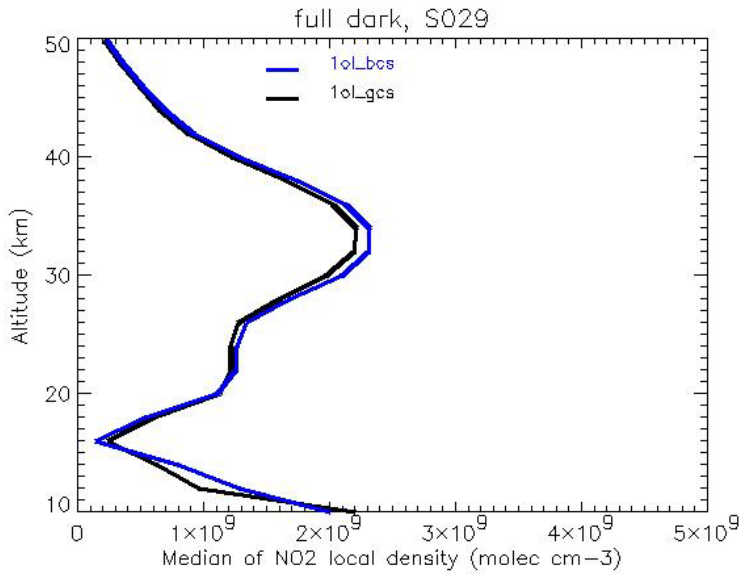

Figure 6.1-5: Vertical profile of the median of NO_2 local density (blue: configuration with Bremen cross-sections; black: configuration with GOMOS cross-sections). Results are based on a dataset of 567 dark limb occultations at low latitudes

There is small impact on air (a very slight decrease of the air median local density between 15km and 23km for some datasets). For a 1/λ law aerosol model, there is an increase of the median aerosol extinction coefficient below 22km (up to 10% and more locally) due to the change of cross-sections (results at low latitudes shown on fig. 6.1-6; fig. 6.1-2); this increase is not observed with a 2nd degree aerosol model.

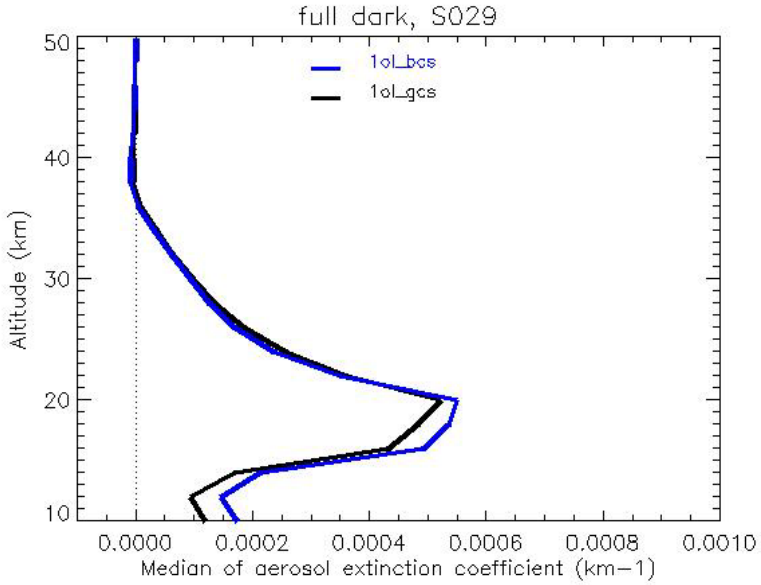

Figure 6.1-6: Vertical profile of the median of the aerosol extinction coefficient (blue: configuration with Bremen cross-sections; black: configuration with GOMOS cross-sections). Results are based on a dataset of 567 dark limb occultations at low latitudes

There is very small change on the dispersion of the local density or of the aerosol extinction coefficient profiles due to the change of cross-sections.

The impact on χ^2 profiles is small (fig. 6.1-2). The misfits in the median of the residuals are decreased for some altitude levels (20km, 30km) when compared to the ones from the configuration with GOMOS cross-sections (fig. 6.1-7 to be compared to fig. 6.1-8).

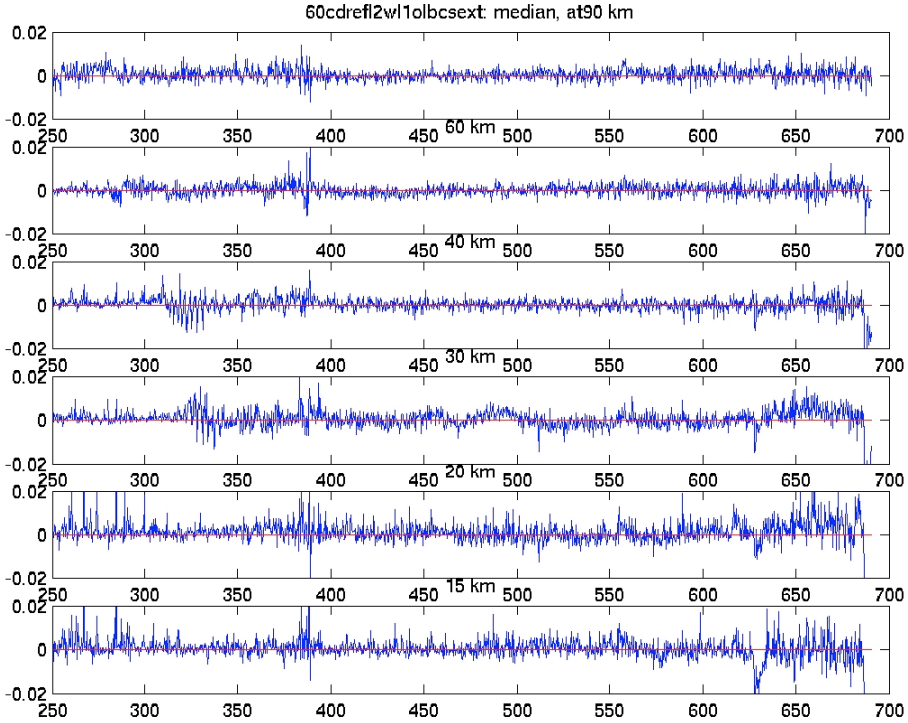

Figure 6.1-7: Median of the residual values at several altitude levels between 90km and 15km for the configuration with Bremen cross-sections (1/λ law for the aerosol model). Results are based on a dataset of 241 dark limb occultations at various latitudes

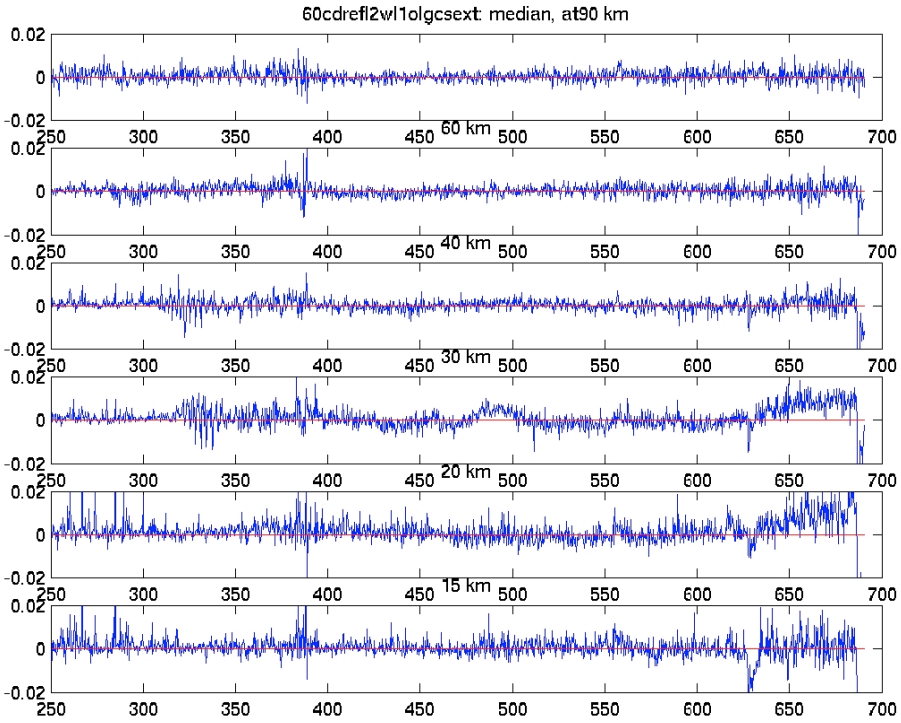

Figure 6.1-8: Median of the residual values at several altitude levels between 90km and 15km for the configuration with GOMOS cross-sections (1/λ law for the aerosol model). Results are based on a dataset of 241 dark limb occultations at various latitudes

6.1.3.2.2 Impact of the choice of aerosol model

The use of a 1st degree polynomial instead of a (1/λ) law for the aerosol model produces in average higher O_3 local densities between 20km and 40km; small positive values of the difference between median profiles at almost every altitude level in this range are obtained. There are also hints of lower O_3 values at low altitudes for some datasets.
The aerosol extinction coefficient shows an increase between 10km and 35 km (positive values of the difference between median profiles in this altitude range).
The relative difference between median profiles of χ^2 shows small negative values of a few %, indicating a small average decrease of the χ^2 values when the 2nd degree polynomial instead of the 1/λ law is used for the aerosol model.

The comparison between results from configuration with "free air" and air fixed to ECMWF values (for a 2nd degree polynomial aerosol model) shows that the median value of NO_2 local density is increased below 15km.
There is a large effect on the median value of the aerosol extinction coefficient which is highly increased below 22km; it shows positive values of the median below 14km instead of negative ones obtained with "free air" (fig. 6.1-9).
The dispersion of O_3 is slightly decreased in a large range of altitudes; and the dispersion of the aerosol extinction coefficient is decreased at all altitudes when air is fixed (fig 6.1-9).

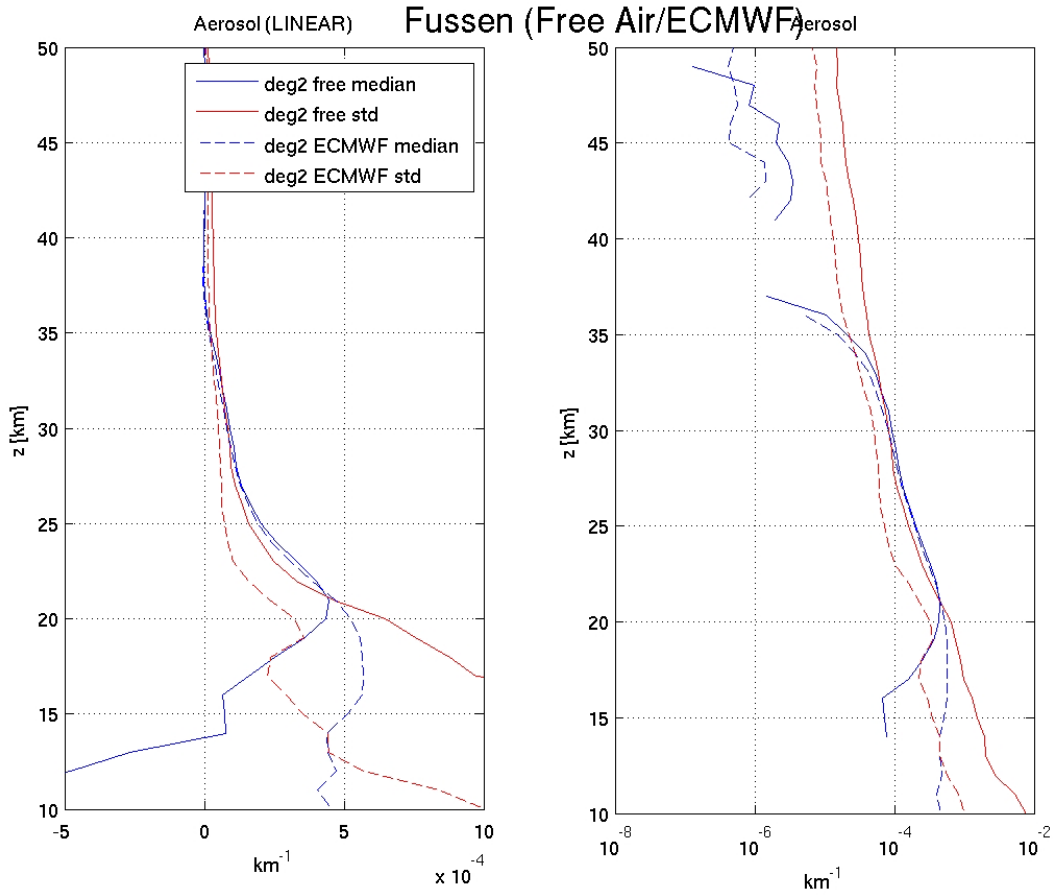

Figure 6.1-9: Vertical profiles of the median and of the standard deviation of the aerosol extinction coefficient for 2nd degree polynomial configuration, with "free" air and air fixed to ECMWF values, linear scale (left) and logarithmic scale (right). Results are based on a dataset of 589 dark limb occultations at various latitudes

The comparison of O_3 vertical profiles with external measurements shows that there is a negative effect of the 2nd degree aerosol model when the air density in the retrieval is not constrained by ECMWF values.

The use of a 2nd degree polynomial instead of a $1/\lambda$ law for the aerosol model (air now fixed to ECMWF values and use of GOMOS cross-sections) increases the median value of O_3 local density at the maximum level and also in a greater extent at low altitudes (results at low latitudes shown on fig. 6.1-10). The relative difference between the median values of the O_3 local densities shows positive values between 13km and 40km (fig. 6.1-11).

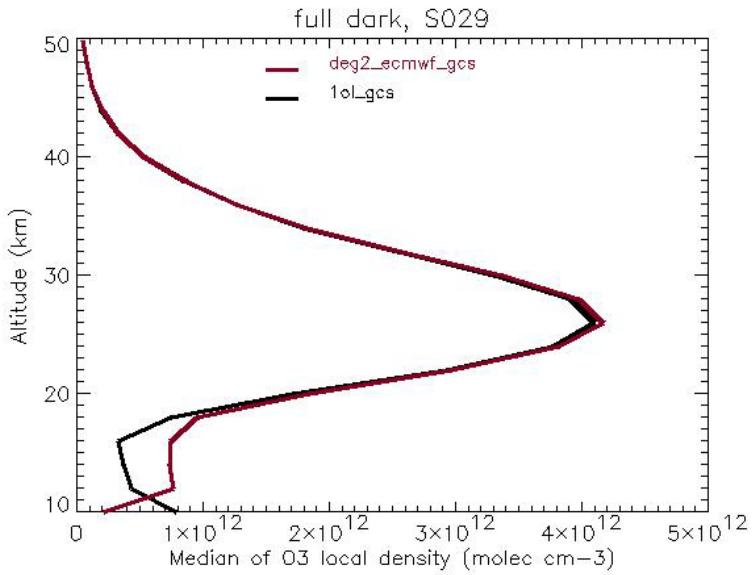

Figure 6.1-10: Vertical profile of the median of the aerosol extinction coefficient (blue: configuration with Bremen cross-sections; black: configuration with GOMOS cross-sections). Results are based on a dataset of 567 dark limb occultations at low latitudes

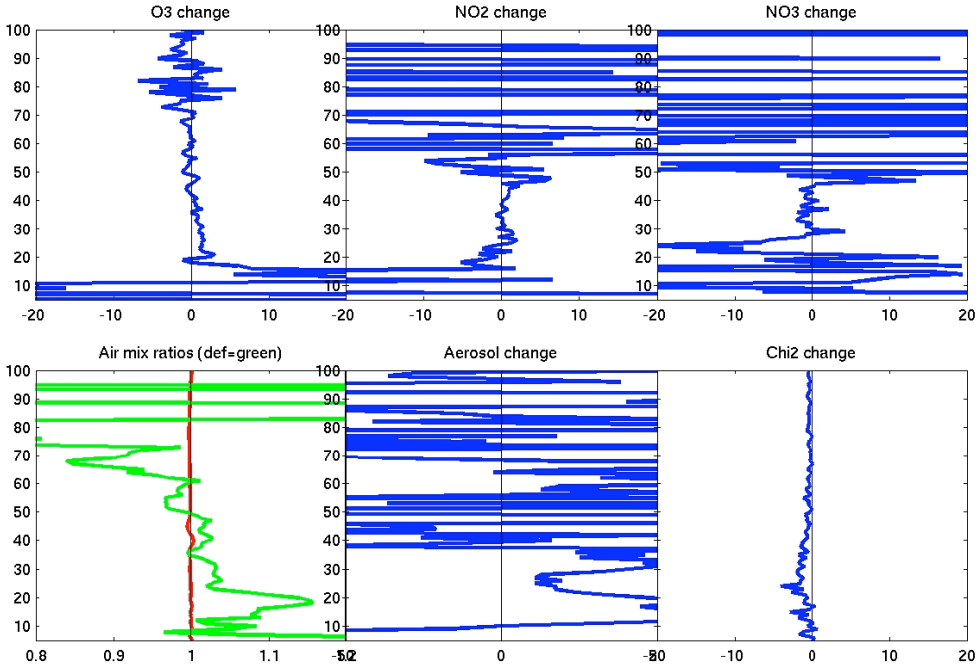

Figure 6.1-11: Comparison between two different configurations: 2nd degree polynomial and 1/λ law for the aerosol model (GOMOS cross-sections). Results are based on a dataset of 241 dark limb occultations at various latitudes. Top row: Vertical profiles of the relative difference ("2nd degree polynomial" – "1/λ law") between median of O_3, NO_2, NO_3 local densities by the two configurations (2nd degree polynomial - 1/λ law). Bottom row: Vertical profiles of the air mixing ratio by the two configurations, of the relative difference between median of the aerosol extinction coefficient, and of the relative difference between the median of the χ^2 values from the two configurations

There is a small increase effect on the median vertical profiles of the NO_2 local density at low altitudes.
An increase of the aerosol extinction coefficient with the 2nd degree polynomial is observed (results at low latitudes shown on fig. 6.1-12) with large positive values of the difference between median profiles between 15km and 35km at least (fig. 6.1-11).

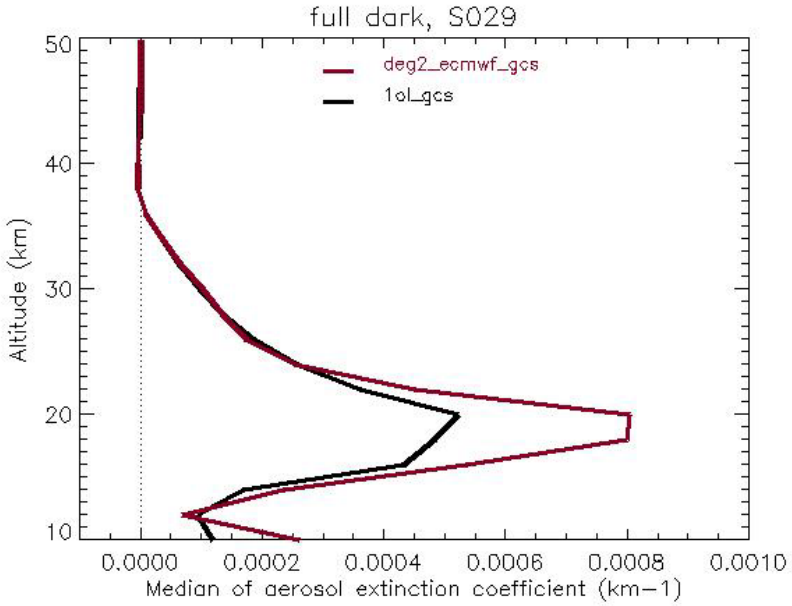

Figure 6.1-12: Vertical profile of the median of the aerosol extinction coefficient (red: configuration with 2nd degree polynomial aerosol model; black: configuration with 1/λ law for the aerosol model). Results are based on a dataset of 567 dark limb occultations at low latitudes

The dispersion of O_3 local density profiles is increased below 15km (low latitudes). The dispersion of NO_2 local density profiles is decreased below 20km. There is also a decrease of the dispersion of the aerosol extinction coefficient (extent of the altitude range depending on datasets) with the 2nd degree polynomial aerosol model.
The relative difference between median profiles of χ^2 shows small negative values of a few %, indicating a small average decrease of the χ^2 values (fig. 6.1-11). The misfits in the median of the residuals are decreased with the 2nd degree aerosol model for some altitude levels (20km, 30km) when compared to the ones from the configuration with GOMOS cross-sections (fig. 6.1-13 to be compared to fig 6.1-8).
However, more profiles are rejected for bad quality criteria (too few points, non-defined values, no altitude overlap with ground-based measurements, large error bars...) with the 2nd degree polynomial than with the 1/λ aerosol law.

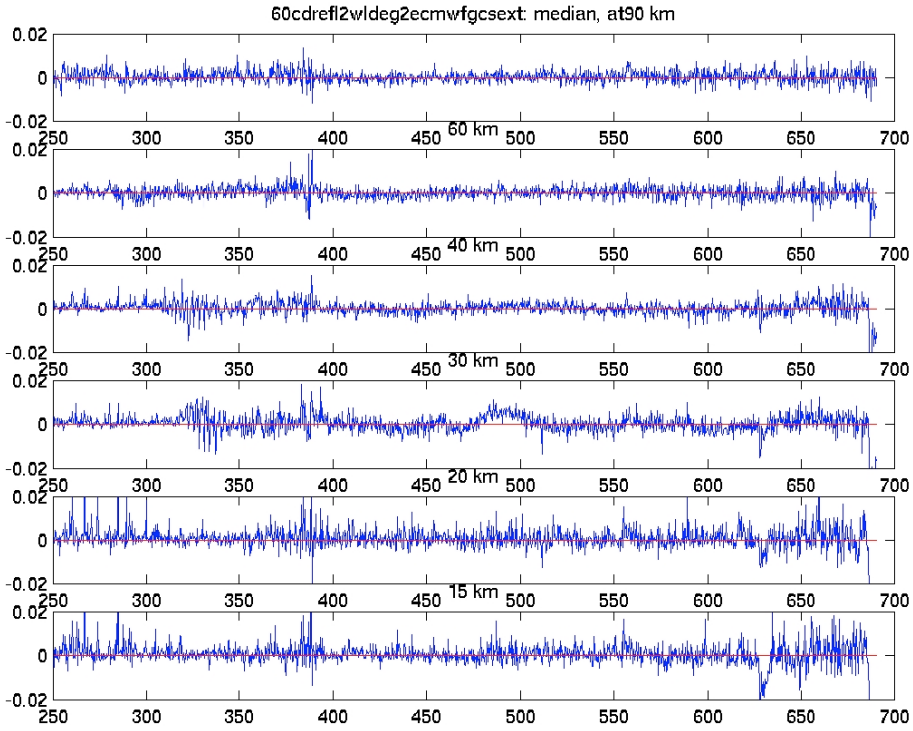

Figure 6.1-13: Median of the residual values at several altitude levels between 90km and 15km for the configuration with 2nd degree polynomial aerosol model (GOMOS cross-sections). Results are based on a dataset of 241 dark limb occultations at various latitudes

6.1.3.2.3 Conclusions

From the various results for those different test versions, it has been decided by QWG to use a second degree polynomial for the aerosol model, to fix air to ECMWF values, and to use Orphal cross-sections for O_3 and GOMOS cross-sections for NO_2. This will be the baseline configuration for the retrieval of GOMOS measurements in the frame of the second reprocessing operations and also for the next upcoming IPF processor version GOMOS/5.00.

6.2 Quality Flags Monitoring

In this section it is plotted some information contained in the Quality Summary data set of the level 2 products of September 2005. In particular, it is depicted the percentage of flagged points per profile for the local species O_3, H_2O, NO_2 and Air. Only products in dark limb illumination conditions and without fatal errors (error flag in the MPH set to "0") are used.

A profile point in a level 2 product is flagged when:

- The local density is less than a given minimum value
- The local density is greater than a given maximum value
- A negative local density was found

- The line density is not valid. And it occurs when:
  - The acquisition from level 1b is not valid
  - There is no acquisition used for reference star spectrum
  - The line density is less than a given minimum value
  - The line density is greater than a given maximum value
  - A negative line density was found

  For species: air, aerosol, O_3, NO_2, NO_3, OClO
  - No convergence after a given number of LMA iterations
  - χ^2 out of LMA is bigger than χ^2
  - Failure of inversion

  For species: O_2, H_2O
  - Spectro B only: no convergence
  - Spectro B only: data not available
  - Spectro B only: covariance not available

There are points mainly between -40° and +55° latitude because in this period of the year full dark illumination condition occultations (only those products have been used for these plots) are found on that region. In summer, full dark illumination data are mainly in the Southern Hemisphere while in winter it is the contrary: full dark illumination occultations are found mainly in the Northern Hemisphere.

Looking at the fig. 6.2-1 the most evident characteristic that can be observed is the high percentage of flagged points per profile for H_2O. Users should not use these data, as their quality is still poor. The percentage of flagged points per profile for O_3 and Air is around 35% whereas for NO_2 it becomes 60%. It can be seen also that there are latitudinal bands with almost the same color (same percentages). This means that the percentages of flagged points per profile have a dependence on the stars that have been observed: a given star is always observed at the same latitude but at different longitude.

In fig. 6.2-2 it is depicted the same information as in fig. 6.2-1 but for given specie **valid altitude ranges** (see table 6.2-1), that is, altitude ranges where data with the best quality should be found. For O_3 the percentage of flagged points per profile is small between 20 and 60 Km altitude. For NO_2 it becomes less than 20 % for altitudes between 20 and 50 Km and for Air profiles, the percentage of flagged points is small for altitudes between 25 and 45 Km. For H_2O, considering the whole profiles or considering points below 50 Km does not change the high percentage of flagged points. In the SAA the percentages of flagged points per profile are slightly higher than in the rest of the world for O_3, NO_2 and Air.

Table 6.2-1: Valid altitude ranges

Specie	O_3	NO_2	Air	H_2O
Valid altitude range (km)	20 - 60	20 - 50	25 - 45	< 50

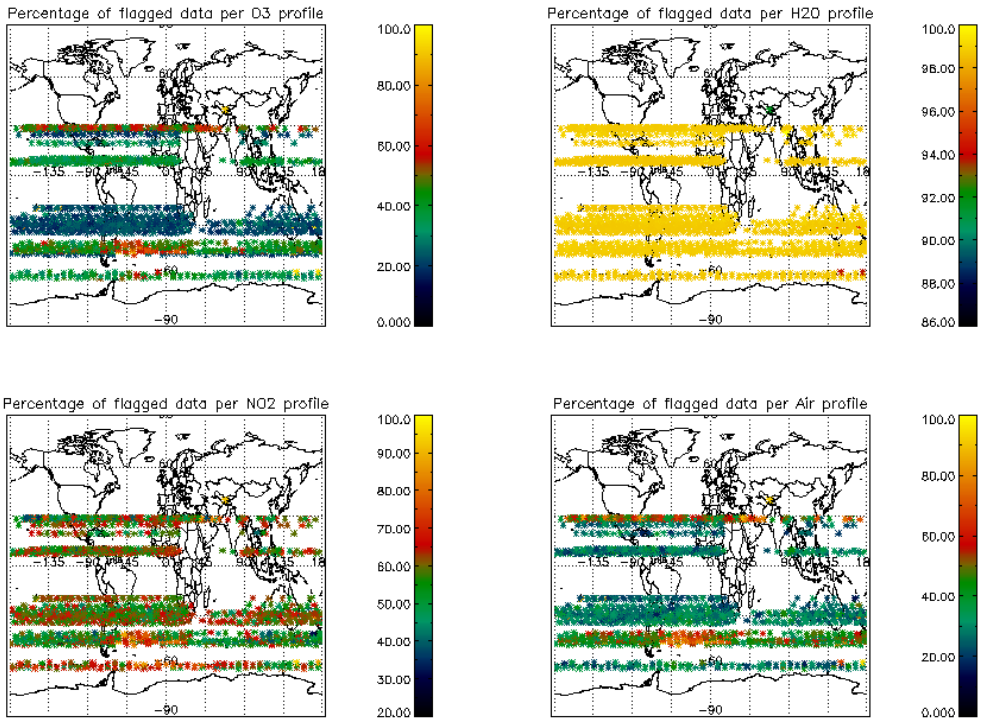

Figure 6.2-1: Percentage of flagged points per profile

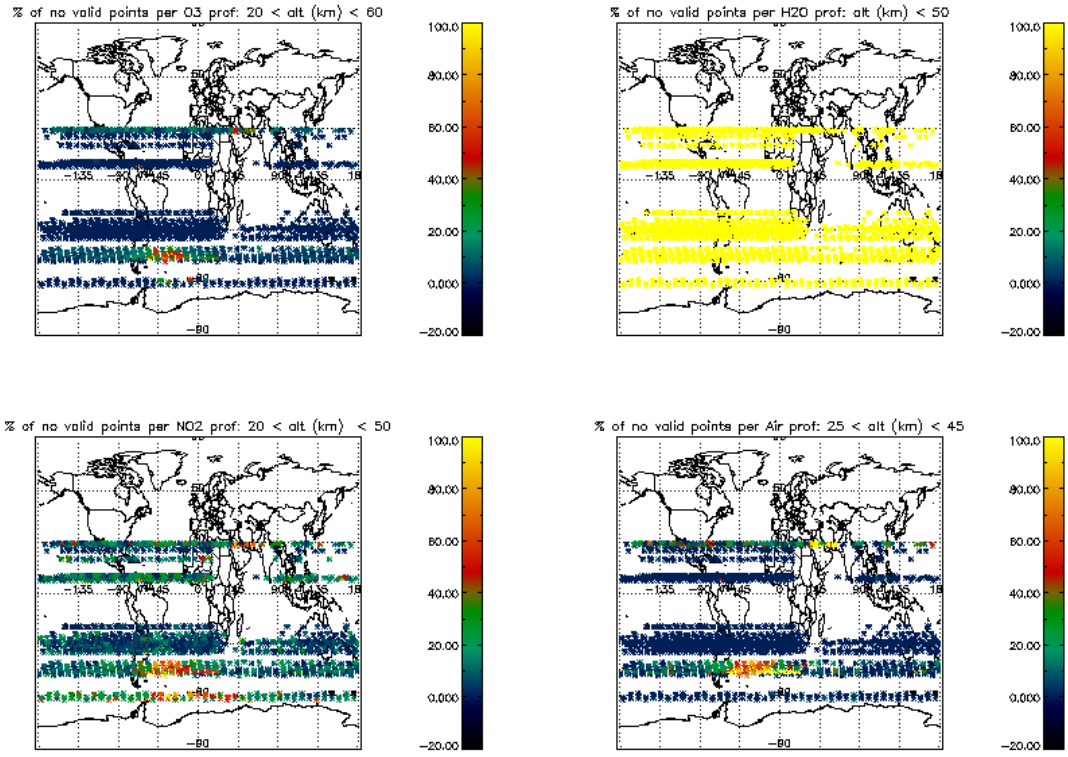

Figure 6.2-2: Same as fig. 6.2-1 but for valid altitude ranges of table 6.2-1

6.3 Other Level 2 Performance Issues

The plot presented in fig. 6.3-1 is the average of the Ozone values during September 2005 in a grid of 0.5 degrees in latitude per 1 km in altitude. Only occultations in dark limb have been used. Even if there is a clear reduction on latitude coverage due the restricted azimuth field of view of the instrument, still some known characteristics can be seen:

- O_3 concentrations show a decrease with latitude near 40 km altitude. In the lower latitudes O_3 is generated by photolysis of O_2
- In the middle stratosphere (25-30 km) O_3 is strongly influenced by transport effects. Strong meridional and zonal transport is visible in middle and higher latitudes
- The lower stratosphere shows an O_3 increase with latitude. Highest values can be found within the polar regions due to downward transport of rich air masses

However, other characteristics seem not to be realistic as the values below 15 km, where data are not reliable at the moment.

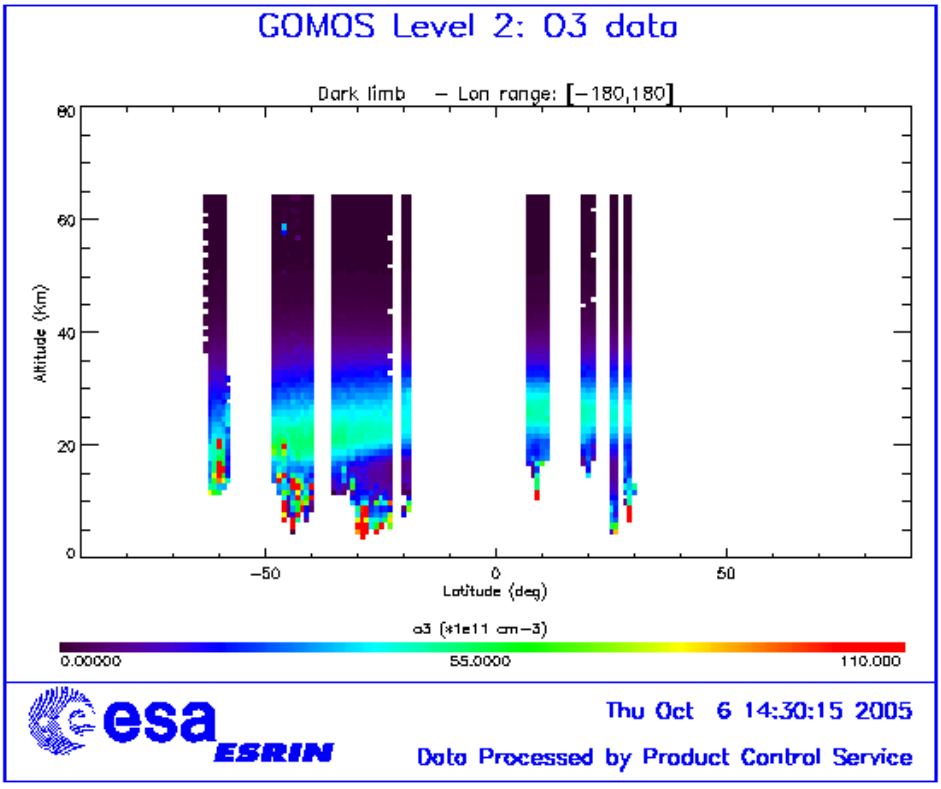

Figure 6.3-1: Average GOMOS O_3 profile during September 2005: average in a grid of 0.5° latitude x 1 km altitude

7 VALIDATION ACTIVITIES AND RESULTS

7.1 GOMOS-ECMWF Comparisons

7.1.1 TEMPERATURE AND OZONE COMPARISONS

Due to restrictions in the current METEO product format, filtering of METEO data is not possible. ECMWF results are therefore partially based on data that are not to be used for scientific application, as mentioned in the disclaimer (http://envisat.esa.int/dataproducts/availability/disclaimers)

7.1.1.1 August 2005

Warning: GOMOS was declared operational since 29 August 2005, even if there are ECMWF reports also for July and August data.

Summary of ECMWF GOMOS monthly report for August data (GOM_RR__2P):

- Availability of GOMOS NRT ozone and temperature data at ECMWF resumed on 18 July
- No data between 12 and 18 August
- Overall good agreement between GOMOS and ECMWF temperatures
- GOMOS temperatures are lower than ECMWF temperatures in most of the stratosphere and lower mesosphere, but area mean departures are less than 1% in most of the stratosphere. Larger departures are found in the mesosphere in particular above 0.4 hPa
- Large differences between GOMOS and ECMWF ozone values (over 50% in places)
- Large scatter of GOMOS ozone data
- Scatter plots still show some unrealistically low GOMOS ozone values
- Data gap data between 5S and 20S
- No water vapour data in NRT GOMOS BUFR files
- The monitoring statistics were produced with the operational ECMWF model, CY29R2

The full August 2005 ECMWF report can be found in the link below:
http://earth.esa.int/pcs/envisat/tmp_calval_res/2005/ecmwf_gomos_monthly_200508_all.pdf

7.1.1.2 September 2005

Summary of ECMWF GOMOS monthly report for September data (GOM_RR__2P):

- Overall good agreement between GOMOS and ECMWF temperatures
- GOMOS temperatures are lower than ECMWF temperatures in most of the stratosphere and lower mesosphere, but mean departures are less than -2 K in the global mean. Larger departures are found in the mesosphere in particular above 0.2 hPa
- Large differences between GOMOS and ECMWF ozone values (over 50% in places)
- Large scatter of GOMOS ozone data

- Scatter plots show some unrealistically low and high GOMOS ozone values
- No data or very few data at all levels/layers between about 40N-20S/30E-180E
- Poor data coverage below 80 hPa in particular in the tropics and at high latitudes
- No water vapour data in NRT GOMOS BUFR files
- The monitoring statistics were produced with the operational ECMWF model, CY29R2

The full September 2005 ECMWF report can be found in the link below:
http://earth.esa.int/pcs/envisat/tmp_calval_res/2005/ecmwf_gomos_monthly_200509_all.pdf

7.2 GOMOS-Climatology comparisons

Results will be presented upon availability.

7.3 GOMOS Assimilation

Results will be presented upon availability.

7.4 Consistency Verification: GOMOS-GOMOS Inter-comparison

Results will be presented upon availability.

7.5 Inter-Comparison with external data

Results will be presented upon availability.